



universität
wien

DIPLOMARBEIT

Titel der Diplomarbeit

„IRES-mediated Translation of Laminin B1 during
Hepatocellular Epithelial to Mesenchymal Transition“

Verfasserin

Nicole Them

angestrebter akademischer Grad

Magistra der Naturwissenschaften (Mag.rer.nat.)

Wien, 2011

Studienkennzahl lt. Studienblatt:

A 490

Studienrichtung lt. Studienblatt:

Diplomstudium Molekulare Biologie

Betreuerin / Betreuer:

Ao. Univ.-Prof. Mag. Dr. Wolfgang Mikulits

1 TABLE OF CONTENTS

1	<u>TABLE OF CONTENTS</u>	3
2	<u>ABSTRACT</u>	5
3	<u>ZUSAMMENFASSUNG</u>	6
4	<u>INTRODUCTION</u>	7
4.1	Comparison of epithelial and mesenchymal cells	7
4.2	An overview of epithelial to mesenchymal transition (EMT)	7
4.3	EMT in cancer	9
4.4	Signaling in EMT	10
4.5	EMT in hepatocellular carcinoma (HCC)	11
4.6	TGF- β signaling in cancer	13
4.7	PDGF signaling in cancer	15
4.8	Cap-dependent translation and its role in cancer	17
4.9	Cellular IRES-mediated translation and its role in cancer	18
4.10	Signaling pathways regulating translation	19
4.11	Laminin B1 (LamB1) mRNA and IRES	20
4.12	La enhances LamB1 IRES translation upon EMT	22
4.13	Working hypothesis and aim of the thesis	24
5	<u>MATERIALS AND METHODS</u>	26
5.1	Cell lines	26
5.2	Cell culture	27
5.3	Vector for bicistronic assays	28
5.4	Transient transfection	30
5.5	Preparation of cell extracts	30
5.6	RNA isolation	31
5.7	Reverse transcription (RT)	31
5.8	Quantitative polymerase chain reaction (qPCR)	32
5.9	β -Galactosidase assay	32
5.10	CAT ELISA	33
5.11	Calculations for bicistronic assays	33

5.12	Bradford assay and Western blot sample preparation	34
5.13	Western blot	35
5.14	Reverse transcriptase (RT)-PCR	38
5.15	Agarose gel electrophoresis	38
<u>6</u>	<u>RESULTS</u>	<u>39</u>
6.1	LamB1 IRES translation is controlled by MAPK and PI3K pathway	39
6.2	MAPK pathway predominantly regulates LamB1 expression in epithelial hepatocytes	41
6.3	PI3K and MAPK pathway regulate LamB1 expression in mesenchymal hepatocytes	45
6.4	EMT-transformed cells activate PDGF signaling	46
6.5	PDGF controls cytoplasmatic La accumulation and LamB1 IRES translation upon EMT	48
6.6	Further investigation of PDGF downstream signaling	50
<u>7</u>	<u>DISCUSSION</u>	<u>52</u>
7.1	Concluding remarks and future perspectives	58
<u>8</u>	<u>REFERENCES</u>	<u>60</u>
<u>9</u>	<u>ANNOTATION</u>	<u>69</u>
<u>10</u>	<u>CURRICULUM VITAE</u>	<u>70</u>
<u>11</u>	<u>ACKNOWLEDGEMENTS</u>	<u>71</u>

2 ABSTRACT

Translation of cellular mRNAs is most frequently started by the cap-dependent scanning mechanism. However, another initiation process directly recruits ribosomes to a RNA motif located within the 5'-untranslated region (5'-UTR), referred to as internal ribosome entry site (IRES). Several IRES-containing mRNAs have important roles during tumor progression. The epithelial to mesenchymal transition (EMT) represents a crucial mechanism of hepatocellular carcinoma development, which is caused by the synergy of transforming growth factor (TGF)- β and oncogenic Ras, involving an upregulation of platelet-derived growth factor (PDGF) signaling. Interestingly, elevated translation of the extracellular matrix component laminin B1 (LamB1) was observed during hepatocellular EMT. The increase of LamB1 was found to depend on an IRES element located in the 5'-UTR of its mRNA. Furthermore, the IRES trans-acting factor La showed accumulation in the cytoplasm and was identified to bind and enhance LamB1 IRES activity upon EMT. In this study we analyzed the signaling pathways regulating LamB1 IRES translation during hepatocellular EMT. We employed different murine hepatocyte cell lines expressing oncogenic Ras or mutant versions of Ras subeffector signaling. Additionally, we performed pharmacological interference in murine hepatocytes. Our results suggest that mainly the mitogen-activated protein kinase (MAPK) pathway controls LamB1 IRES translation in epithelial hepatocytes and that upon EMT the MAPK as well as the phosphatidylinositol 3-kinase (PI3K) pathway regulate the LamB1 IRES translation. Moreover, the data indicate that the MAPK pathway is the major regulatory pathway of LamB1 IRES during hepatocellular EMT. Further investigations showed that PDGF signaling enhances LamB1 IRES activity by controlling cytoplasmic La localization in EMT-transformed hepatocytes. Therefore, we propose that the PDGF signaling enhances MAPK and PI3K signaling as well as cytoplasmic La localization, which upregulates LamB1 IRES translation upon hepatocellular EMT.

3 ZUSAMMENFASSUNG

Die Initiation der Translation zellulärer mRNAs wird von einem „Scanning“-Mechanismus reguliert, welcher von der Präsenz der m⁷G-Cap-Struktur am 5'-Terminus der mRNA abhängig ist. Zusätzlich gibt es einen Prozess, bei dem Ribosomen innerhalb der 5'-untranslatierten Region (5'-UTR) direkt an ein RNA-Motiv, dem sogenannten „internal ribosome entry site“ (IRES), binden. Zelluläre mRNAs mit IRESs spielen eine wichtige Rolle in der Tumorprogression. Die epitheliale-mesenchymale Transition (EMT) von Hepatozyten nimmt eine Schlüsselrolle in der Tumorentwicklung ein und wird durch die Kooperation von „Transforming Growth Factor“ (TGF)- β und onkogenem Ras induziert. Diese EMT-transformierten Zellen weisen nicht nur einen verstärkten „Platetelet-Derived Growth Factor“ (PDGF) Signalweg, sondern auch eine vermehrte Translation der Laminin B1 (LamB1) mRNA auf. Ein IRES innerhalb der LamB1 5'-UTR ist für die Hochregulierung dieser extrazellulären Matrixkomponente verantwortlich. Während der EMT neoplastischer Hepatozyten akkumuliert der IRES trans-aktivierende Faktor La im Zytoplasma und bindet an den LamB1 IRES um seine Translation zu verstärken. In dieser Arbeit haben wir Signalwege analysiert, welche die LamB1 IRES Translation regulieren. Wir untersuchten Zelllinien maligner Hepatozyten, die onkogenes Ras oder mutierte Versionen von Ras Subeffektor Signalwegen exprimieren. Zusätzlich verwendeten wir pharmakologische Inhibitoren in Maushepatozyten. Unsere Ergebnisse deuten darauf hin, dass primär der „Mitogen-Activated Protein Kinase“ (MAPK) Signalweg die LamB1 IRES Translation in epithelialen Hepatozyten kontrolliert und dass nach der EMT sowohl der MAPK als auch der „Phosphatidylinositol 3-Kinase“ (PI3K) Signalweg die LamB1 IRES Translation erhöhen. Zusätzlich weisen unsere Daten darauf hin, dass der MAPK Signalweg der Hauptregulationsweg für die LamB1 IRES Translation während der hepatozellulären EMT ist. Weitere Untersuchungen zeigten, dass der PDGF Signalweg die La Akkumulation im Zytoplasma kontrolliert und dadurch die LamB1 IRES Aktivität in EMT-transformierten Hepatozyten erhöht. Daraus schließen wir, dass der PDGF Signalweg während der hepatozellulären EMT nicht nur die MAPK und PI3K Signalwegaktivierung steigert, sondern auch zu einer Akkumulation von La im Zytoplasma führt, welche eine Erhöhung der LamB1 IRES Translation bewirkt.

4 INTRODUCTION

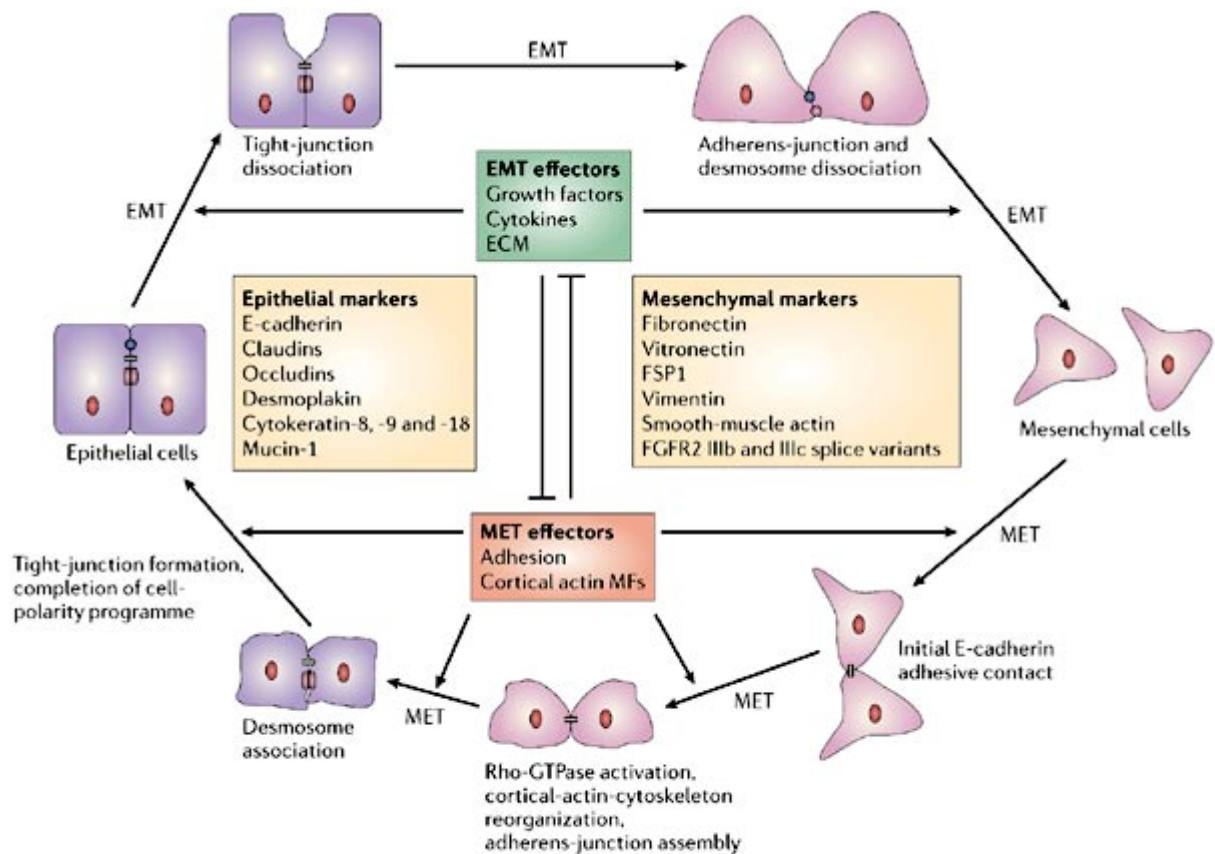
4.1 Comparison of epithelial and mesenchymal cells

Epithelial cells connect to each other to form polarized layers [1]. The basal lamina, also referred to as basement membrane, is an extracellular matrix (ECM) located at the basal side of epithelial structures [2]. Its main components, laminins and collagen IV, form a meshwork that gives mechanical support, separates epithelial cells from connective tissue, serves as barriers for epithelial cell movement into connective tissue and regulates cell polarity, differentiation as well as migration [2]. Epithelial cells bind to the ECM via heterodimeric integrins that are connected to the intracellular cytoskeleton [3]. Notably, integrins influence migration, cell proliferation and survival [3]. Tight junctions close intercellular gaps, hinder diffusion of molecules and support apical/basolateral polarity, whereas gap junctions facilitate exchange of small molecules from cell to cell [4]. Direct cell-cell adhesions are based on cadherins, which are Ca^{2+} -dependent homophilic transmembrane proteins [5]. An adhesion belt is formed via contacts of cadherins with actin filaments by β -catenin and additional anchor proteins [4]. Desmosome junctions facilitate mechanical strength of epithelia [6]. They are formed by cadherins, which are linked to intermediate filaments over adaptor proteins like desmoplakin [6]. Epithelial cells mainly express E-cadherin whereas fibroblasts or nerve cells express N-cadherin [4, 7]. Cadherins are important for contact guidance and tissue assembly during embryonic development [4].

In contrast to epithelial cells, mesenchymal cells are neither polarized nor arranged in cell layers [1]. However, mesenchymal cells can have a front-back polarity [8]. Cultured epithelial cells form clusters whereas fibroblast-like mesenchymal cells appear spindle-shaped [1]. Mesenchymal cells are normally partly attached to their neighbors, but not linked to a basal lamina and therefore often involved in cell migration [1].

4.2 An overview of epithelial to mesenchymal transition (EMT)

EMT describes the change of highly organized epithelial cells to migratory mesenchymal cells [9]. This conversion is mediated by complex alterations in cell signaling and architecture (Figure 1). EMT is reversible by the process termed mesenchymal to epithelial transition (MET). Typical epithelial markers are for instance E-cadherin as well as the intermediate filament proteins cytokeratin-8, -9 and -18 [9]. Mesenchymal markers include the ECM component fibronectin, the intermediate filament vimentin and smooth-muscle actin [9].



Copyright © 2006 Nature Publishing Group
Nature Reviews | Molecular Cell Biology

Figure 1 Epithelial cells convert into mesenchymal cells by EMT and vice versa via MET [9]. Diverse effectors, which influence junctional complexes, and typical markers are outlined.

EMT is involved in (1) morphogenesis, (2) tissue homeostasis, (3) disease and (4) (cancer) stemness (Figure 2) [10]. (1) For example, during embryogenesis, EMT is essential for the development of the three-layered embryo, a process known as gastrulation [11]. In mice, fibroblast growth factor (FGF) signaling regulates the expression of the transcriptional repressor Snail, which in turn blocks E-cadherin transcription [11]. Furthermore, previous to offspring formation, neural crest cells have to pass through EMT to migrate, which is partly mediated by Snail [12]. Snail-induced EMT was also reported to be involved in cardiac valve development in the chick [13]. (2) During wound healing, transcriptional repressor Slug-mediated partial EMT enables keratinocytes to migrate into de-epithelialized area [14]. (3) ECM deposition by elevated numbers of myofibroblasts is a characteristic of fibrosis [15]. Fibroblasts accumulating in the connective tissue have been shown to partially derive from EMT-transformed epithelial cells [15]. For example, inflammatory signaling mediated by transforming growth factor- β (TGF- β) and FGF induces EMT in the kidney [15].

Interestingly, inflammation triggers tumor necrosis factor- α (TNF- α)-mediated EMT during fibrosis or cancer [16]. EMT has a major role in tumor progression, which it is particularly outlined below in 4.3. (4) Recently it was proposed that EMT-transformed cells gain stemcell-like properties [17]. For instance, the EMT-involved transcriptional repressor Zeb1 is associated with tumor cell stemness [18].

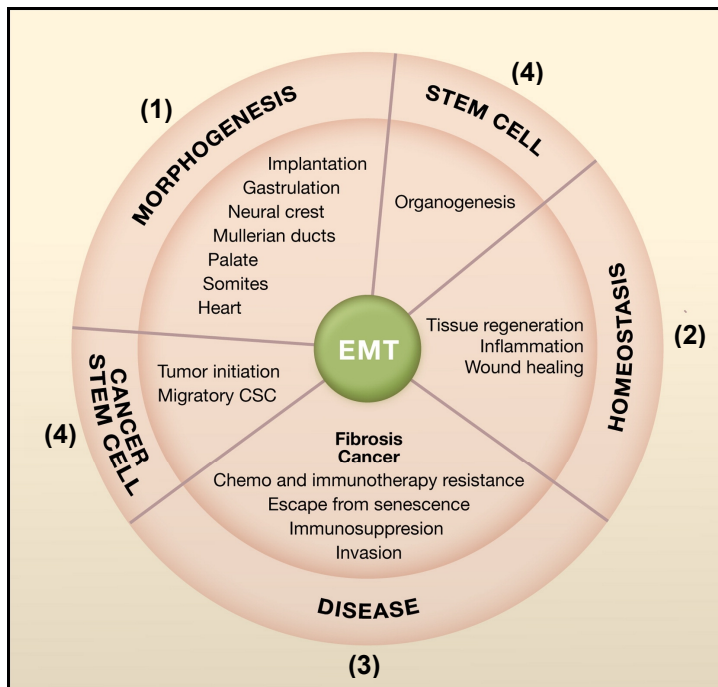
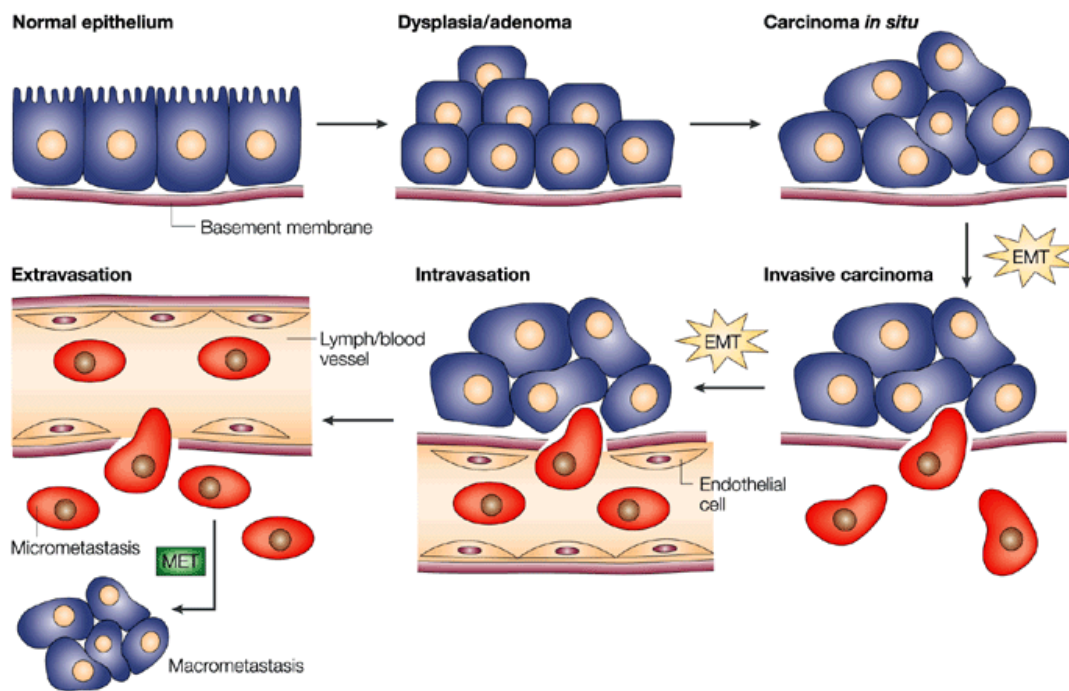


Figure 2 EMT plays a role in (1) morphogenesis, (2) tissue homeostasis, (3) disease and (4) (cancer) stemness. Adapted from [10].

4.3 EMT in cancer

One hallmark of cancer is tissue invasion and metastasis, which causes most human cancer deaths [19, 20]. Cancer cells escape from primary tumors by migrating either collectively or individually as amoeboid cells or mesenchymal cells [21]. The latter ones are derived from epithelial cells that have undergone EMT [10]. Figure 3 shows a scheme of invasion and metastasis driven by EMT and MET in carcinoma cells [22]. The key pathway for EMT induction is TGF- β signaling as discussed in 4.6 [23]. Notably, EMT is not only implicated in cancer cell dissemination but also in resistance to oncogene-induced premature senescence [24]. The EMT-involved transcriptional repressors Twist 1 and 2 protect cells from senescence by inhibition of p21 and p16. Furthermore, EMT correlates with resistance to chemotherapy and is suggested to be involved in immune-suppressive and -resistance mechanisms [10, 25].



Nature Reviews | Cancer

Figure 3 EMT and MET drive tumor progression in carcinoma [22]. Polarized epithelial cells (blue) are connected to basement membrane. Local proliferation results in adenoma formation, which further develops to a carcinoma *in situ* by additional transformation. The carcinoma *in situ* is still surrounded by an intact basement membrane. Local invasion is characterized by EMT and basement membrane fragmentation. Mesenchymal cells (red) intravasate into blood or lymph vessels to colonize distant organs. After extravasation cancer cells undergo MET in order to form micro or -macrometastases.

4.4 Signaling in EMT

EMT is regulated by same or related signaling pathways during physiological and pathological events [10]. An excerpt of central pathways influencing EMT is outlined in Figure 4. Extracellular signals, including ECM constituents such as hyaluronic acid or soluble growth factors such as TGF- β and FGF, regulate EMT [26-28]. Hepatocellular growth factor (HGF) for instance transduces signals via the receptor tyrosine kinase (RTK) c-Met and the mitogen-activated protein kinase (MAPK) cascade to downregulate E-cadherin expression [29]. Furthermore, growth factors such as FGF can signal via phosphatidylinositol-3'-kinase (PI3K), which is an essential pathway for EMT [30]. Notch signaling was also described to play a role during EMT [31]. In addition, microRNAs and hypoxia were reported to control EMT [32, 33].

Notably, most EMT inducers and pathways downregulate E-cadherin expression, which is fundamental for EMT [22]. Downregulation of E-cadherin is achieved amongst others by transcriptional repression and promoter hypermethylation [34]. Important transcriptional repressors include the zinc finger proteins Snail and Slug, homodomain/zinc finger proteins Zeb1 and Zeb2 as well as basic helix-loop-helix (bHLH) proteins E12/E47 and Twist [34]. Notably, E-cadherin protein expression or activity can be lost by mutations as well [35]. Loss of E-cadherin leads to the dissociation of epithelial junctions [9]. As a consequence, β -catenin translocates to the nucleus where it acts as a co-activator for TCF4/LEF to induce Wnt signaling. Not only cell-cell but also cell-matrix junctions are remodeled during EMT. $\alpha\beta1$ integrins are for instance necessary for collagen and FGF1-mediated EMT [36].

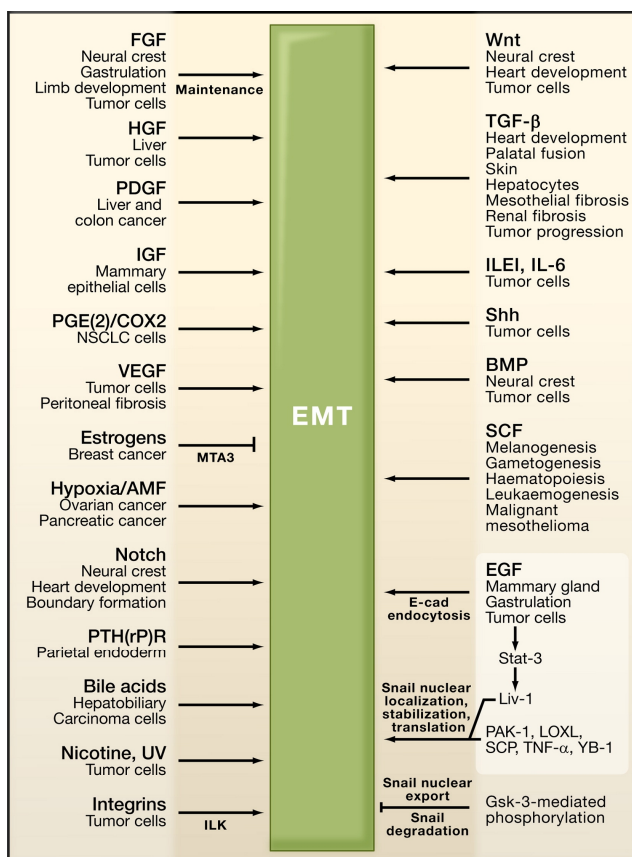


Figure 4 Overview of signaling pathways regulating EMT [10]. Biological processes are shown with their matching EMT inducing signals.

4.5 EMT in hepatocellular carcinoma (HCC)

HCC is a primary liver cancer, which is generally caused by chronic liver disease and cirrhosis [37]. The main reasons for HCC are hepatitis B, hepatitis C, alcoholic liver disease and nonalcoholic steatohepatitis [37]. Further risk factors of HCC are aflatoxin, obesity, diabetes mellitus and predispositions like hemochromatosis [37]. HCC is frequently

diagnosed at advanced stages of disease and curative treatments include liver resection or liver transplantation [38, 39]. In an immunohistochemical analysis it was observed that E-cadherin and β -catenin levels are frequently decreased in HCC patients [40]. This downregulation significantly correlated with tumor progression, intrahepatic metastasis and reduced patient survival. Another study of HCC patients revealed that increased levels of Snail, Slug and the ECM component laminin-5 associated with decreased E-cadherin levels and nuclear translocation of β -catenin [41].

To investigate the molecular mechanisms of hepatocellular EMT, a murine EMT tumor model was established (Figure 5). Immortalized murine $p19^{ARF/-}$ hepatocytes (termed MIM) undergo EMT by the cooperation of constitutive active Ras and TGF- β signaling [42, 43]. EMT-transformed hepatocytes acquire an autocrine loop of TGF- β signaling, leading to the activation of platelet-derived growth factor (PDGF) signaling and increased malignancy (for a detailed view see Figure 15) [42, 44].

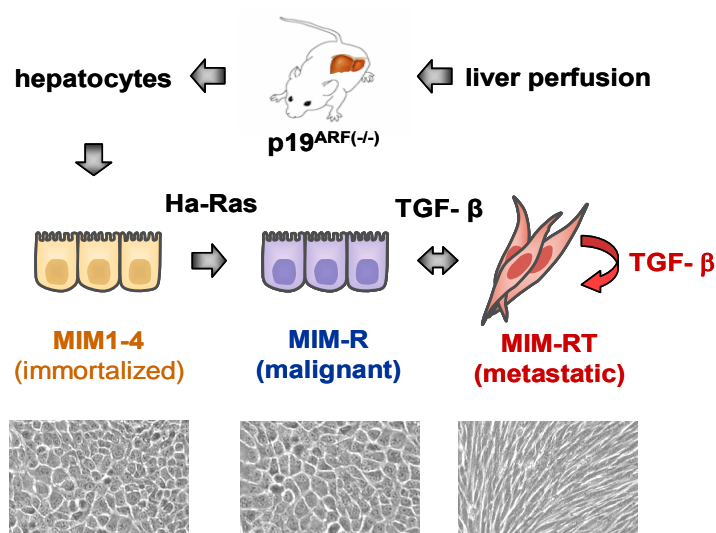


Figure 5 The hepatocellular EMT model. Immortalized MIM-1-4 hepatocytes were established after liver perfusion of $p19^{ARF/-}$ mice [43]. These epithelial cells grow in monolayers and are non-tumorigenic. Stable transmission of MIM-1-4 cells with oncogenic v-Ha-Ras gave rise to MIM-R cells [42]. These cells show still a polarized epithelial morphology but are tumorigenic. Long-term TGF- β -treatment of MIM-R induces hepatocellular EMT resulting in MIM-RT cells [42]. These cells have a mesenchymal phenotype and grow in polylayers without contact inhibition. Importantly, MIM-RT cells form metastases and are therefore more malignant than MIM-R. Phase contrast images are adapted from [42].

4.6 TGF- β signaling in cancer

TGF- β signaling has fundamental roles during tumor development and progression since it influences cell survival, proliferation and invasion [45]. Remarkably TGF- β signaling shows both tumor suppressive as well as promoting functions [46]. TGF- β ligands (TGF- β 1, - β 2 and - β 3) bind serine/threonine kinase TGF- β type 1 and 2 receptors (TGFBR1 and TGFBR2, respectively) to initiate signaling [47]. TGF- β ligands are expressed in latent forms and need to be activated by proteolytic cleavage or structural modifications [48]. Upon activation they bind specifically to TGFBR2, inducing heterotetramerization of receptors and phosphorylation of TGFBR1 by TGFBR2 (Figure 6) [47]. TGFBR1 in turn becomes active and recruits as well as phosphorylates receptor-regulated Smads (R-Smads) [47]. Active R-Smads interact with common partner Smad (co-Smad) that facilitate nuclear translocation [47]. Smads form complexes with additional transcription factors and regulate gene expression [47]. TGF- β controls besides canonical Smad signaling also non-Smad pathways such as PI3K and MAPK pathways [49].

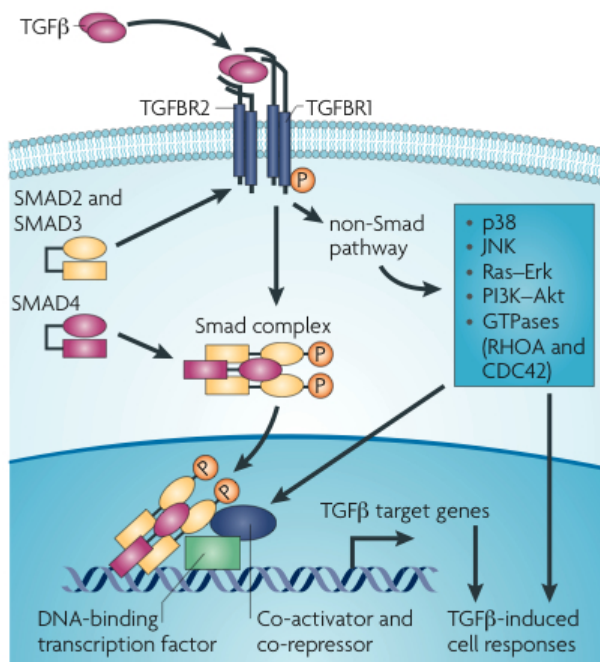


Figure 6 TGF- β signal transduction [46]. The receptors are activated upon binding to TGF- β resulting in phosphorylation of R-Smads (SMAD2 and 3) and formation of the Smad-complex (R-Smad and co-Smad, SMAD4) that translocates to the nucleus. TGF- β target genes are regulated through interaction of Smad-complexes with DNA-binding factors and co-factors. Additionally, non-Smad pathways can be activated.

On the one hand several findings suggest that TGF- β acts as a tumor suppressor, for instance TGFBR2 and SMAD4 are frequently inactivated [50]. Furthermore, TGF- β blocks cell proliferation by regulating cyclin-dependent kinase inhibitors (CDKIs) and MYC expression [51, 52]. TGF- β antagonists like c-Ski and SnoN bind SMAD3 and 4, thus counteract tumor suppressive TGF- β effects [53]. Moreover, TGF- β is able to induce apoptosis by activating downstream targets such as death-associated protein kinase (DAPK) [54]. Recently it was reported that TGF- β signaling transcriptionally activates autophagy genes (ATG) in certain hepatocellular carcinoma, which mediates autophagy and growth arrest [55]. In some cancers TGF- β inhibits angiogenesis, for example in diffuse-type gastric carcinoma it increases the expression of the angiogenic inhibitor thrombospondin 1 (TSP1) [56].

On the other hand TGF- β has tumor promoting features. It stimulates proliferation through activation of PDGF pathway in diverse mesenchymal and cancer cells [57, 58]. Moreover, it has an anti-apoptotic function by inducing the transcription factor Differentially Expressed in Chondrocytes 1 (DEC1) [59]. Recently, TGF- β was suggested to be involved in the regulation of cancer stem cells (CSCs), which are a subpopulation of cancer cells with stem cell features and elevated ability to initiate tumors [46, 60]. Furthermore, tumor angiogenesis is positively influenced by TGF- β through the activation of regulators like vascular endothelial growth factor (VEGF) [61].

As mentioned earlier, TGF- β activates signaling pathways, which are essential during EMT [23]. TGF- β leads to the downregulation of proteins that mediate tight junctions and adherens junctions [62]. Main transcription factors and their function in TGF- β -mediated EMT are displayed in Figure 7. Moreover, TGF- β induces the expression of Mdm2, which in turn destabilizes p53 [63].

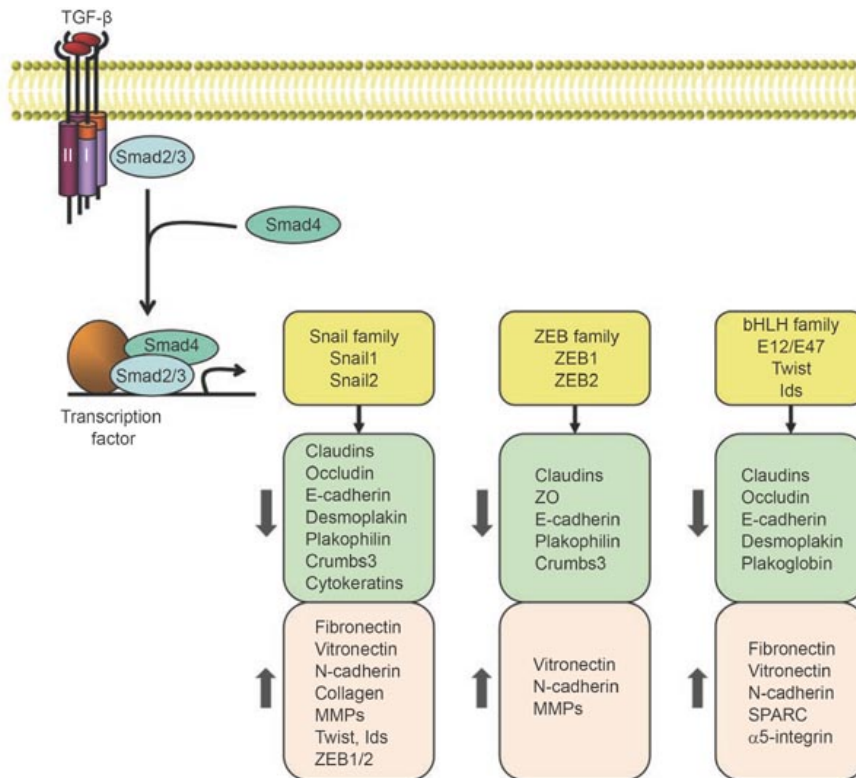


Figure 7 TGF-β-regulated transcription in EMT [62]. TGF-β activated Smads control transcription of target genes by interactions with other transcription factors. The additional transcription factors belong to the Snail, ZEB and bHLH family, listed in yellow boxes. Repressed epithelial markers are indicated in green boxes and enhanced mesenchymal markers are shown in pink boxes.

Overall, the cell type as well as the cellular context defines TGF-β signaling [46]. TGF-β acts as a tumor suppressor during initial steps of tumor development whereas it has tumor promoting functions through cancer progression [64].

4.7 PDGF signaling in cancer

PDGF ligands (PDGF-A, -B, -C, -D) form generally homodimers, with PDGF-AB being the exception [65]. The RTKs PDGF-Rα and -Rβ homo- or heterodimerize upon ligand binding, leading to autophosphorylation and activation [66]. Downstream signal transduction is mediated by the Ras-MAPK cascade or phospholipase C-γ (PLC-γ), which positively influence cell growth and migration [67, 68]. PI3K signaling is another pathway downstream of PDGF that mediates cell movement and growth as well as inhibition of apoptosis [69, 70]. Further reported PDGF pathways include Src, signal transducers and activators of transcription (STATs) as well as integrins [67]. PDGFs and its receptors are expressed in

specific patterns depending on the cell type and stimuli [65]. For instance, epithelial cells display PDGF-A expression, whereas vascular endothelial cells PDGF-B, pericytes PDGF-R β and mesenchymal cells PDGF-R α expression. Furthermore, hypoxia induces PDGF-A, -B and -R β expression in liver [71].

PDGFs are often expressed in cancer cells to support tumor progression (Figure 8) [66]. Paracrine PDGF signaling acts on tumor stroma such as pericytes and cancer-associated fibroblasts (CAFs) [72]. For instance, it was reported that increased numbers of pericytes stabilize tumor vessels [72]. Furthermore, excessive PDGF signaling leads to pericyte detachment and elevated metastasis [73]. CAFs recruited by PDGF signaling were shown to enhance tumor growth, dissemination and angiogenesis through CXCL12, CCL5 and VEGF, respectively [74-76]. Autocrine PDGF signaling enhances EMT in colon carcinoma by the translocation of β -catenin to the nucleus [77].

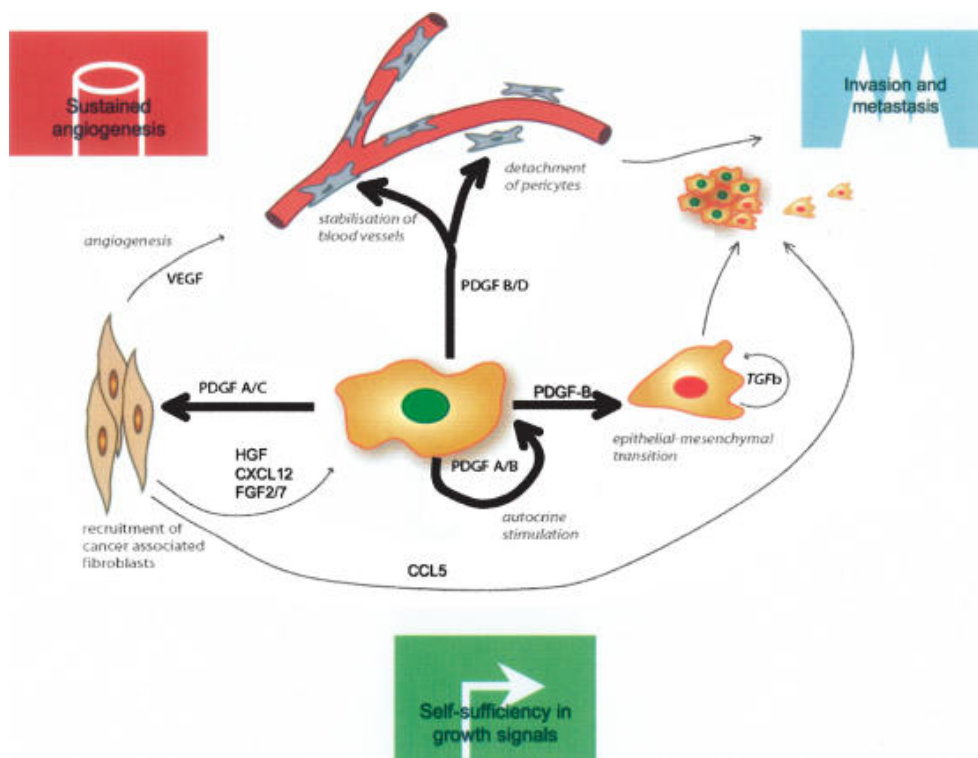


Figure 8 PDGF in tumor progression [65]. Autocrine PDGF signaling enhances EMT in tumor cells. PDGF-A, C secretion engages cancer-associated pericytes and fibroblasts. The latter ones enhance tumor growth, dissemination and angiogenesis through factors like CXCL12, CCL5 and VEGF, respectively [74-76]. Vessel stabilization and pericyte detachment, which promote metastasis, are influenced by PDGF-B and -D [65]. Thick arrows indicate direct effects.

4.8 Cap-dependent translation and its role in cancer

Translation of mRNA consists of four steps that are initiation, elongation, termination and ribosome recycling [78, 79]. Initiation is well known as being the rate-limiting step [78, 79]. The majority of mRNAs is translated by a cap-dependent mechanism where the eukaryotic initiation factor 4F (eIF4F) complex binds to the 7-methyl guanosine (m^7G) cap of the mRNA (Figure 9) [80]. The eIF4F complex includes the cap-binding protein eIF4E, the scaffolding protein eIF4G and the RNA helicase eIF4A. eIF4G interacts with polyA tail binding protein (PABP), leading to mRNA circularization and enables ribosome recycling [80]. The small ribosomal subunit (40S), the ternary complex consisting of eIF2, GTP and Met-tRNA_i, form together with eIF3, eIF1 and eIF1A the 43S initiation complex [80]. eIF3 interacts with eIF4G, which recruits the 43S initiation complex to the mRNA, initiating ribosome scanning for a suitable AUG initiation codon along the 5'-end [80]. eIF1 and eIF1A enable start codon recognition and the presence of AUG will lead to eIF2-bound GTP hydrolysis, large (60S) ribosomal subunit joining, 80S ribosome formation and translational initiation [80].

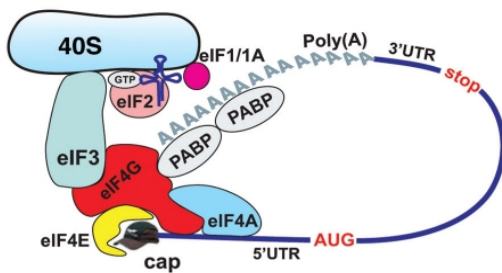


Figure 9 A simplified view of translational initiation by the cap-dependent mechanism. eIF4F complex binds to the capped 5'-end of the mRNA, leading to small subunit binding, ribosome scanning and translational initiation. Adapted from [81].

Translation is often deregulated during cancer development and progression. For instance, translation in tumor cells is unaffected by hypoxia-mediated inhibition [82]. Furthermore, overexpression of eIF4E enhances amongst others HCC and B cell lymphomas [83]. Interestingly, eIF4E inhibitory binding proteins (4E-BPs) regulate the accessibility of eIF4E [84]. Hypophosphorylated (active) 4E-BPs remove eIF4E from eIF4F complex and impede cap-dependent translation. Reduced 4E-BPs expression or augmented 4E-BPs phosphorylation was linked to tumor progression and decreased survival [84].

4.9 Cellular IRES-mediated translation and its role in cancer

Investigations of viral gene expression revealed an alternative translational initiation mechanism [85]. Transcripts that harbor a highly structured motif, referred to as internal ribosome entry site (IRES), allow direct binding of the 40S ribosomal subunit and cap independent translation (Figure 10) [86]. Cellular IRESs are predominately located in the 5'-untranslated regions (5'-UTRs) of mRNAs, however, they have no shared sequence or structural motifs [81]. Highly structured 5'-UTRs hinder efficient ribosome scanning, thus cap-dependent translation [81]. IRESs within such 5'-UTRs allow translation of these mRNAs. Furthermore, cellular IRESs allow constant translation of specific mRNAs during conditions when cap-dependent translation is downregulated [81]. Such conditions include amino acid starvation, endoplasmic reticulum stress, hypoxia, mitosis, cell differentiation, growth arrest and apoptosis. Notably, several of these stress conditions play an important role during cancer [19, 87]. IRES elements are regulated by canonical initiation factors of translation (eIFs) and IRES trans-acting factors (ITAFs) (Figure 10). It is suggested that most IRESs do not need eIF4E or eIF4G, which is cleaved under stress conditions [88]. For instance, c- and N-myc IRES activity does not depend on eIF4E and eIF4G, but still requires eIF4A and eIF3 [89]. In contrast, c-Src kinase mRNA was shown to bind directly to 40S ribosome [90]. ITAFs are RNA binding proteins that typically have a wide range of functions beside the regulation of internal initiation [91]. Nevertheless, they do not directly influence cap-dependent translation [92]. Many ITAFs are able to shuttle between nucleus and cytoplasm, which regulates their activity [93]. However, little is known about mechanisms regulating cellular IRES, which provides an interesting target for future studies.

IRES-mediated translation influences tumorigenesis through IRES regulated mRNAs, the corresponding polypeptides are involved in angiogenesis, cell proliferation and apoptosis [87]. Recent reports describe a hypoxia-activated switch from cap-dependent to -independent translation that is induced by elevated levels of eIF4G1 and 4E-BP-1 during tumor progression [94]. This enhanced tumor size, angiogenesis and survival by IRES translated HIF-1 α , VEGF-A and BCL-2 mRNAs. In multiple myeloma, interleukin-6-induced binding of the ITAF heterogenous nuclear ribonucleoprotein A1 (HnRNPA1) augments IRES-mediated Myc translation leading to the activation of cell proliferation [95]. In non-small-cell lung carcinoma, the anti-apoptotic factor X-linked inhibitor of apoptosis (XIAP) is upregulated by IRES-mediated translation, resulting in resistance to radiation [96].

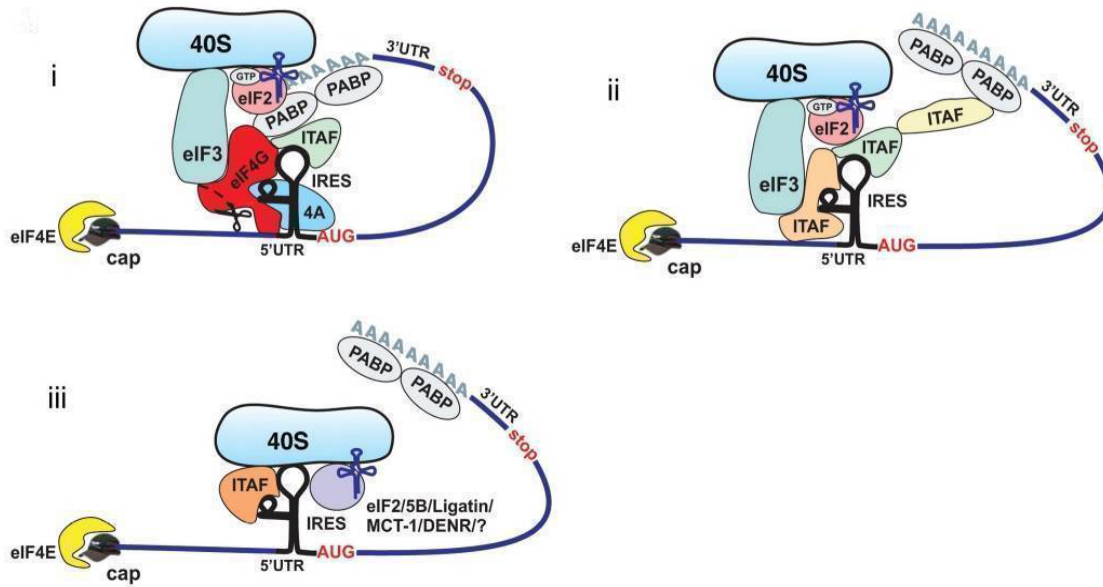


Figure 10 IRES-mediated translational enables 40S ribosome binding without eIF4E and intact eIF4G. Suggested mechanisms: (i) many eIFs and ITAFs are necessary (ii) less eIFs are needed (iii) only ITAFs are required. Adapted from [81].

4.10 Signaling pathways regulating translation

Translation is mainly controlled by the PI3K and MAPK pathway, which are frequently altered in cancer (Figure 11). Mitogenic signals like growth factors, hormones or cytokines activate RTKs that in turn stimulates Ras and PI3K. Activated Ras plays an important role during cancer by activating for example the MAPK cascade Raf (Ras activated factor)-extracellular signal-related kinase (ERK) kinase (MEK)-ERK [97]. Ras recruits Raf in its GTP-bound activated status, which leads to conformational changes and phosphorylation of Raf [97]. Activated Raf in turn phosphorylates and activates MEK, which then phosphorylates and activates ERK [97]. ERK further phosphorylates cytoplasmic substrates as well as transcription factors after nuclear translocation [97]. Erk enhances translation through activation of the downstream targets p90RSK (RSK) and eIF4G-associated kinases MNK1 and 2 [79]. RSK and ERK block tuberous sclerosis 1 (TSC1) and TSC2 GTPase activating protein (GAP), therefore supporting Ras homologue enriched in brain (RHEB)-GTP activation of mTOR complex 1 (mTORC1) [79]. RSK also phosphorylates eIF4B to enhance binding to eIF4A [79]. Activated MNK1 and 2 phosphorylate eIF4E, which promotes translation and tumorigenesis [98].

Activated PI3K phosphorylates phosphatidylinositol (4', 5')-bisphosphate (PIP₂) and creates thereby phosphatidylinositol (3', 4', 5')-trisphosphate (PIP₃) [99]. PIP₃ in turn attracts

proteins exhibiting pleckstrin homology (PH) domains, for example the serine-threonine kinase AKT [99]. Binding and subsequent phosphorylation of AKT leads to its functional activation [99]. AKT acts positively on translation by inhibiting TSC1 and 2 as well as PRAS40 (mTORC1 inhibitor) [79]. TSC1 and 2 are activated by ATP-sensing AMP kinase (AMPK) in response to low ATP levels [79]. mTORC1 promotes cap-dependent translation through inhibition of 4E-BP and activation of ribosomal S6 kinase (S6K) [79]. S6K phosphorylates eIF4B and inhibits programmed cell death protein 4 (PDCD4), which blocks eIF4A [79]. Inhibition of mTORC1 leads to eIF4E sequestration and inactivation of eIF4A as well as eIF4B [79].

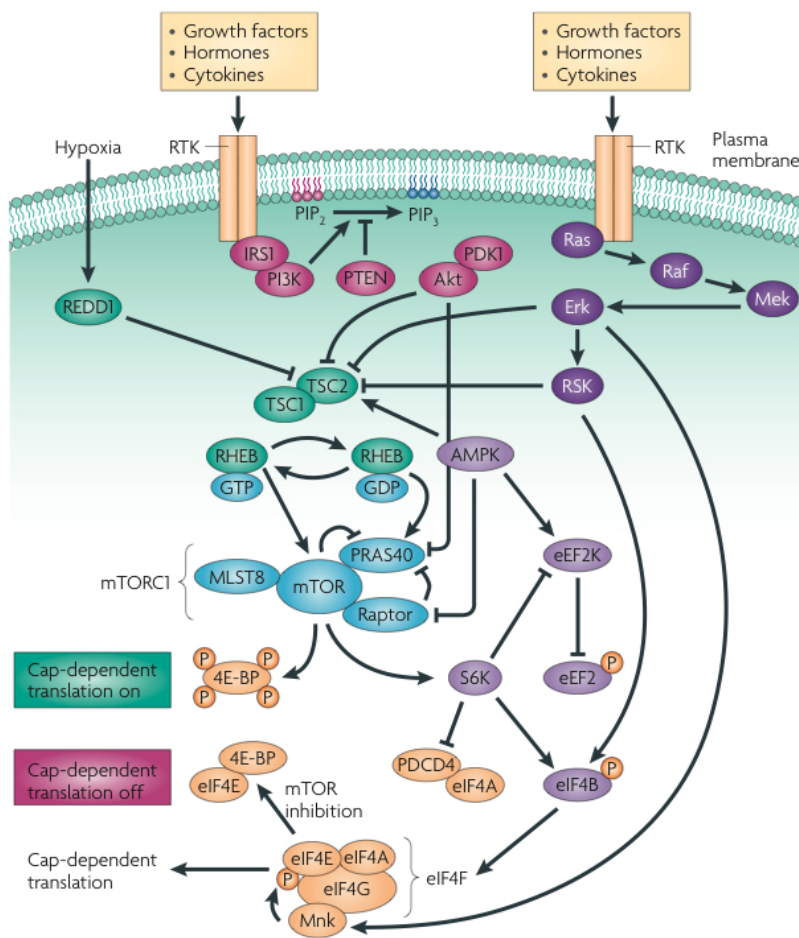


Figure 11 Schematic overview of pathways that control translation [79]. Activated PI3K and MAPK pathways promote hyperphosphorylation of 4E-BP, thereby enhancing translation.

4.11 Laminin B1 (Lamb1) mRNA and IRES

To investigate the role of IRES translation during EMT, a hepatocellular EMT model (Figure 5) was employed that depends on the cooperation of oncogenic Ras and TGF- β [42].

Translational upregulated genes were identified by expression profiling of hepatocellular

EMT comparing polysome-bound to total RNA [100]. Further analysis, such as selection of mRNAs containing unusual long 5'-UTRs, revealed LamB1 to contain a putative IRES [100]. The IRES activity of LamB1 IRES could be verified excluding the presence of cryptic promoter or splice sites within the 5'-UTR [101]. Additionally, the minimal LamB1 IRES sequence was determined [101]. LamB1 IRES activity was measured by bicistronic assays, which revealed an upregulation upon EMT [101]. To our knowledge this is the first described cellular IRES that is controlled upon EMT.

Laminins belong to the class of glycoproteins and are main components of the basement membrane (see 4.1). They are flexible heterotrimers (Laminin $\alpha_x\beta_y\gamma_z$) and LamB1 is one of the three known β -subunits [102]. Notably, LamB1 knock-out is embryonic lethal due to a lack of basement membranes [103]. Laminin chains have common structures like globular and rod-like domains (Figure 12) [104]. Laminin N-terminal domains (LN) are necessary for self-assembly whereas laminin globular domains (LG) mediate interactions with cell surface receptors and ECM constituents [104, 105]. Laminins show a tissue specific distribution and their functions cover basement membrane organization and its anchorage to cells, cell polarization and proliferation [102, 106]. Furthermore, they are implicated in several diseases like epidermolysis bullosa, muscular dystrophy type 1A and cancer [106-108]. Laminins affect cell proliferation, angiogenesis, invasion and metastasis during cancer development [106, 109, 110]. Laminins signal via integrin as well as non-integrin receptors such as α -dystroglycan and 67kDa laminin receptor (LamR) [111, 112]. Recently it has been reported that laminin-511, which contains LamB1 as β -chain, controls breast cancer invasion and metastasis in an integrin-dependent manner [113]. Moreover, it was shown that LamB1 influences laminin-integrin-signaling, which enhances cell adhesion, motility and differentiation [114]. LamB1 was also identified to be involved in endothelial cell adhesion, tube formation and aortic sprouting [115]. Furthermore, LamB1 binds to LamR [116]. LamR is upregulated in several aggressive cancers and correlates with increased invasion and metastasis [117]. For example, LamR interacts with Laminin-111, which contains LamB1 as β -chain, to mediate migration of multiple myeloma cells [118].

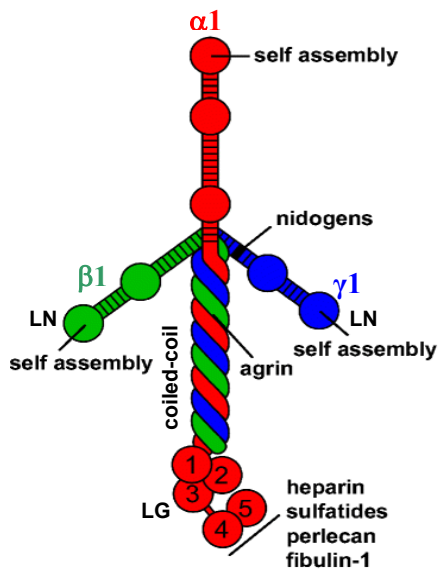


Figure 12 Laminin-111 ($\alpha 1\beta 1\gamma 1$) is shown as an illustration for laminin structure and functions. LNs facilitate self-assembly and LGs bind to ECM molecules like heparin, perlecan as well as fibulin-1. $\gamma 1$ and $\gamma 3$ chains bind to the ECM component nidogen and the coiled-coil domain interacts with the heperan sulfate proteoglycan agrin. Adapted from [104].

4.12 La enhances LamB1 IRES translation upon EMT

Recently we identified La as an ITAF, which binds the LamB1 IRES *in vivo* and *in vitro* [101]. Importantly, we could show that binding of La positively regulates IRES-mediated LamB1 translation [101]. In our hepatocellular EMT model, we did not observe any changes in La protein expression (Figure 13A). However, analysis of cytoplasmic and nuclear cell fractions revealed that most of La is located in the nucleus in MIM-R hepatocytes and that La accumulates in the cytoplasm upon TGF- β treatment as well as EMT (MIM-RT) (Figure 13B). These data indicate that cytoplasmic La accumulation enhances LamB1 IRES translation upon hepatocellular EMT.

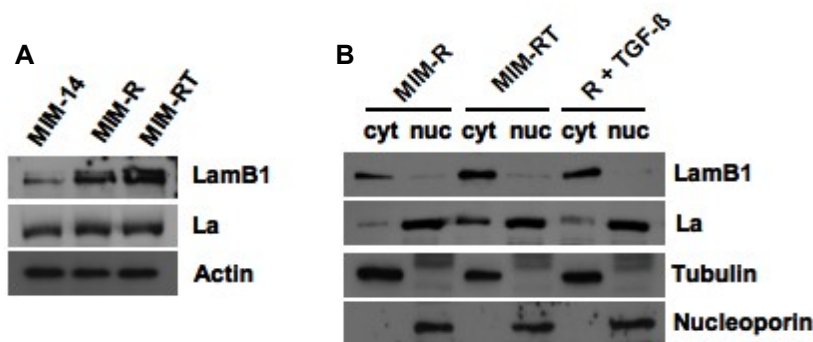


Figure 13 La protein expression in hepatocellular EMT. (A) Total protein levels are not changed upon EMT, (B) whereas cytoplasmic La protein levels increase upon EMT (MIM-RT) and after TGF- β treatment. Adapted from [101].

La is a highly abundant, multifunctional protein, which was discovered as an autoantigen in systemic lupus erythematosus and Sjogren's syndrome [119-121]. The N-terminal domain (NTD) is the most conserved part of La proteins (Figure 14). It includes the La motif and the RNA recognition motif 1 (RRM1) [122]. Another RRM located next to NTD has an unknown function. The region around the short basic motif (SBM) was suggested to be involved in homodimerization [123]. The C-terminus of La proteins is less conserved and highly charged and is the site of phosphorylation as well as cleavage [121, 124-126]. Moreover, the C-terminal nuclear localization signal (NLS) is responsible for nuclear import of La and the nuclear retention element (NRE) causes nuclear accumulation of La [127]. Thus, La is mainly located in the nucleus (nucleoplasmic as well as nucleolar) [128]. Interestingly, it was reported that La can shuttle between nucleus and cytoplasm. Protease cleavage, removing the NLS, and C-terminal phosphorylation by AKT were proposed to mediate cytoplasmic translocation [124, 126, 129]. La is involved in many processes such as pre-tRNA maturation, stabilization of nascent RNAs and regulation of IRES-mediated translation [121]. In summary, La works as an RNA chaperon and ITAF. The ITAF function of La was initially reported in poliovirus-infected cells [130]. It was shown that La redistributes to the cytoplasm upon poliovirus infection where it enhances IRES-mediated poliovirus translation. Notably, cytoplasmic La localization was suggested to be mediated through cleavage of La by a poliovirus-encoded protease [126]. Moreover, it was proposed that homodimerization of La is necessary for enhanced Poliovirus translation [123]. Further translational upregulation by La was described for the cellular IRESs in heavy chain binding protein (BiP), XIAP and cyclin D1 (CCND1) transcripts [131-133]. In addition, one transcript of La harbors an IRES which is thought to lead to an positive feedback loop of La translation during conditions when

cap-dependent translation is impaired [134]. Notably, the study of CCND1 IRES indicated a role of La in cell proliferation and found an overexpression of La in cervical cancer [133].

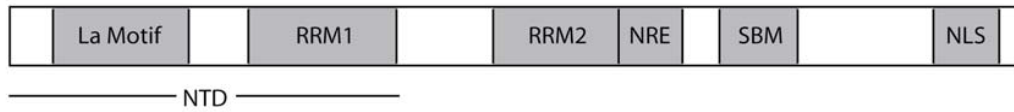
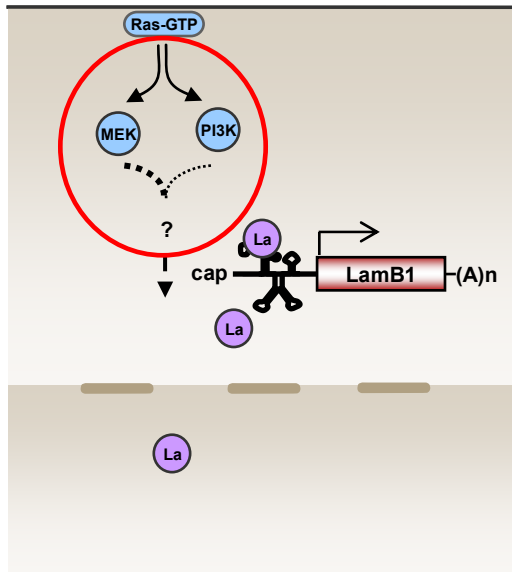


Figure 14 Scheme of the human La protein. Adapted from [122].

4.13 Working hypothesis and aim of the thesis

A working model for the regulation of LamB1 IRES translation during hepatocellular EMT is shown in Figure 15. Epithelial MIM-R hepatocytes expressing constitutive active Ras signal via MAPK or PI3K pathway without additional stimuli [42]. Cytoplasmic La binds to LamB1 IRES to enhance cap-independent translation [101]. Long-term TGF- β treatment of MIM-R cells induces hepatocellular EMT, leading to an activation of autocrine PDGF signaling and increased PI3K and MAPK signaling [42, 44]. Moreover, in EMT-transformed cells elevated levels of cytoplasmic La were shown to enhance LamB1 IRES translation [101]. Activation of PDGF signaling during EMT might regulate LamB1 IRES translation through PI3K or MAPK pathway by stimulating accumulation of cytoplasmic La. The aim of the thesis was therefore to understand which signaling pathways and downstream effectors control LamB1 IRES translation.

Epithelial MIM-R



TGF- β

EMT: mesenchymal MIM-RT

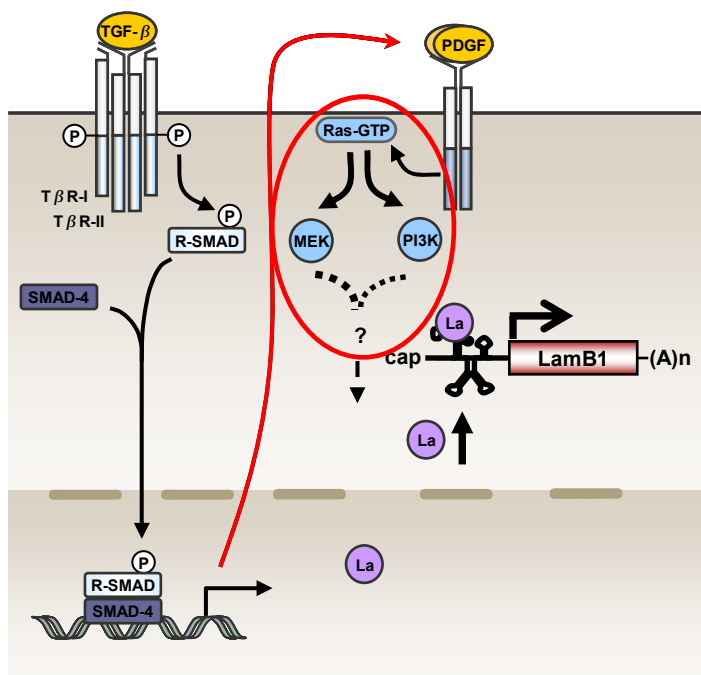


Figure 15 Working model for the regulation of LamB1 IRES translation during hepatocellular EMT. TGF- β signaling cooperates with constitutive active Ras to induce EMT in murine hepatocytes [42]. This in turn activates PDGF signaling and enhances MAPK as well as PI3K pathway activation [42, 44]. Main questions of the study are marked in red: (i) Does MAPK or PI3K pathway regulate LamB1 IRES translation in epithelial and EMT-transformed cells? (ii) Does PDGF signaling control LamB1 IRES translation upon EMT?

5 MATERIALS AND METHODS

5.1 Cell lines

MIM-1-4:

MIM-1-4 cells are immortalized primary hepatocytes isolated from p19^{ARF}^{-/-} mice [43]. These cells are able to undergo Fas-induced apoptosis. Moreover, they possess a non-tumorigenic phenotype and express liver-specific markers such as albumin, hepatocyte nuclear factor-1 α and phenylalanine hydroxylase. MIM-1-4 cells form monolayers and show morphological characteristics of liver parenchyma cells. In culture MIM-1-4 cells need additional growth factor supplying the medium as described.

MIM-R:

MIM-R cells were established by stable retroviral transmission of MIM-1-4 cells with constitutive active, oncogenic v-Ha-Ras and green fluorescent protein (GFP) [42]. These cells show a polarized epithelial morphology, grow in a contact-inhibited fashion and exhibit a malignant phenotype.

MIM-C40:

MIM-C40 cells were established by stable retroviral transmission of MIM-1-4 cells with C40-V12-Ras [42]. This Ras mutant selectively activates PI3K signaling in response to cognate signals. The cells show a polarized epithelial morphology, grow in a contact-inhibited fashion and possess a non-tumorigenic phenotype. Notably, MIM-C40 cells grow slower than MIM-R and MIM-S35 cells (see below) and need additional growth factor supplying the medium as described.

MIM-S35:

MIM-S35 cells were established by stable retroviral transmission of MIM-1-4 cells with S35-V12-Ras [42]. This Ras mutant selectively activates MAPK signaling in response to cognate signals. The cells show a polarized epithelial morphology, grow in a contact-inhibited fashion and are malignant transformed.

MIM-R-dnP:

MIM-R-dnP cells were generated by retroviral transmission of MIM-R with pMSCV-dnPDGF-R α -red, which exhibits red fluorescent protein (RFP) and a dominant negative PDGF-R α [44]. These cells show a polarized epithelial morphology and grow in a contact-inhibited fashion. Compared to MIM-R cells, they have a decreased tumorigenic phenotype.

MIM-RT, -RT-dnP, -ST and -CT:

MIM-RT, -RT-dnP, -ST and -CT cells were established by long-term TGF- β -treatment of MIM-R, -R-dnP, -S35 and -C40 cells, respectively [42, 44]. These cells display a mesenchymal phenotype and grow in polylayers without contact inhibition. MIM-RT and -ST cells show an increased malignancy compared to their corresponding epithelial cells. MIM-RT-dnP cells are less tumorigenic compared to MIM-RT cells and MIM-CT cells need to be cultured with additional growth factor.

5.2 Cell culture

Cultivation of cells:

Murine hepatocyte cell lines were grown on collagen-coated culture dishes (rat-tail collagen, BD Transduction Lab, Franklin Lakes, USA) in RPMI 1640 plus 10% fetal calf serum (FCS) and antibiotics (50 U Penicillin and 50 μ g/ml Streptomycin). To induce EMT, 2,5 ng/ml recombinant human TGF- β 1 (R&D Systems, Minneapolis, USA) was added to the culture medium for 72 hours and constant treatment of epithelial cells with 1 ng/ml TGF- β 1 gave rise to spindle-shaped MIM-RT, -RT-dnP, -CT and -ST cells. MIM-C40 and -CT cells were cultured with extra growth factor supply (GFs), consisting of 20 ng/ml human recombinant transforming growth factor- α (TGF- α , Sigma, St. Louis, USA), 30 ng/ml human recombinant insulin-like growth factor II (IGF-II, Sigma, St. Louis, USA) and 35 ng/ml insulin (Sigma, St. Louis, USA). For Western blot and bicistronic assays after TGF- β treatment, the medium was changed and 2,5 ng/ml TGF- β 1 was applied for 24 hours. For pharmacological treatment, 10 μ M PI3K (LY294002, Cell Signaling, Danvers, USA) and/ or 10 μ M MEK1/2 (UO126, Cell Signaling, Danvers, USA) inhibitor or DMSO (control) was added to the culture medium and cells were harvested 24 hours after incubation. For stimulation were cells serum starved for 24 hours and treated for 30 minutes, 2 hours or 24 hours with either 20 ng/ml PDGF-AB (PeproTech, Rocky Hill, USA), 20% FCS, 40 ng/ml TGF- α or 70 ng/ml insulin. For bicistronic assays after PDGF stimulation, long-term treated cells were cultured with 20 μ M TGF- β -RI/II inhibitor (Lilly, Indianapolis, USA) and 24 hours treated with 10 ng/ml PDGF-

AB. All cells were grown at 37°C and 5%CO₂ and routinely screened for the absence of mycoplasma.

Splitting of cells:

To split cells, the medium was removed and cells were washed with phosphate buffered saline (PBS). Cells were trypsinized with Trypsin/EDTA (0,1% Trypsin/ 0,01% EDTA), resuspended in medium and split in desired ratio onto collagen-coated culture dishes.

Freezing of cells:

To freeze cells, the medium was removed and cells were washed with PBS and trypsinized with T/E. After resuspending cells in medium, they were transferred into a 15 ml Falcon tube. Cells were centrifuged for 6 minutes at 272 g at 4°C and the cell pellet was washed with PBS and centrifuged again. The cell pellet was then resuspended in freezing medium (95% FCS / 5 % DMSO) and transferred into round bottom freezing vials (1 ml suspension/vial). The tubes were immediately placed on ice for 30 minutes and stored at least over night at -80°C. Frozen cells were put at liquid nitrogen for long-term storage.

Thawing of cells:

Frozen cells were quickly thawed in water bath at 37°C, carefully resuspended and put into a 15 ml Falcon tube containing culture medium. After centrifugation for 6 minutes at 272 g, the supernatant was removed and the cell pellet was resuspended in culture medium. The cell suspension was further put onto collagen-coated 6cm culture dishes.

Buffers and solutions:

- 10 x PBS:
 - 80 g NaCl
 - 2 g KCl
 - 11,5 g Na₂HPO₄·2H₂O
 - 2 g KH₂PO₄
 - Fill up with ddH₂O to 1 l and autoclave

5.3 Vector for bicistronic assays

The pβGal/Lam/CAT vector (Figure 16) was cloned to study the IRES activity of LamB1. A schematic overview of the bicistronic reporter expression is given in Figure 17. The first

reporter β -galactosidase (β -Gal) is located behind a CMV promoter and is therefore used to control transfection efficiency and to analyze cap-dependent translation [101]. The second reporter chloramphenicol acetyltransferase (CAT) is located downstream of the LamB1 5'-UTR, thus its translation is mediated by the IRES located within the 5'-UTR.

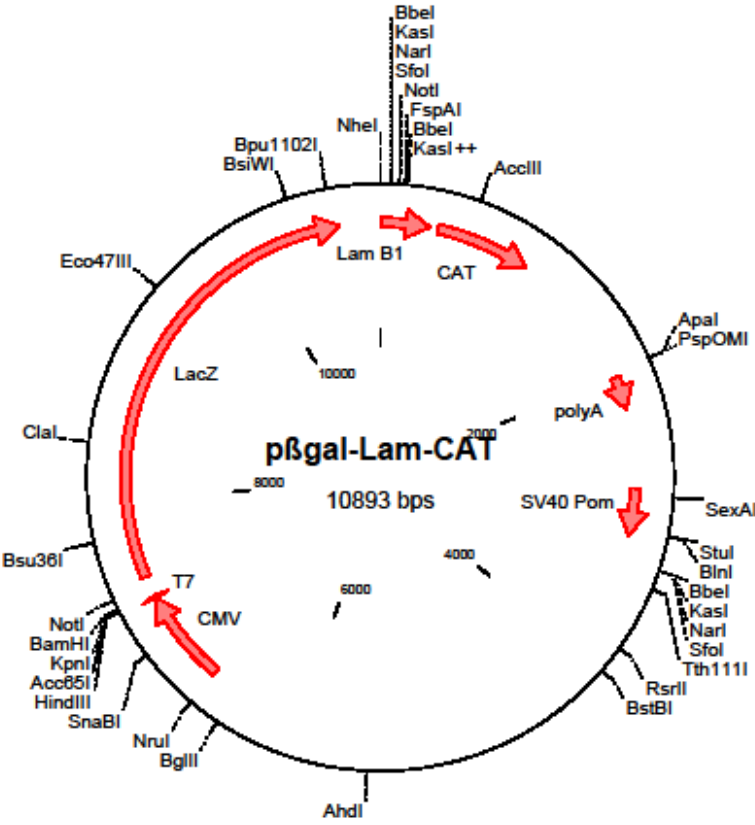


Figure 16 The bicistronic vector p β Gal/Lam/CAT contains the LamB1 5'-UTR located between the two reporters β -Gal and CAT.

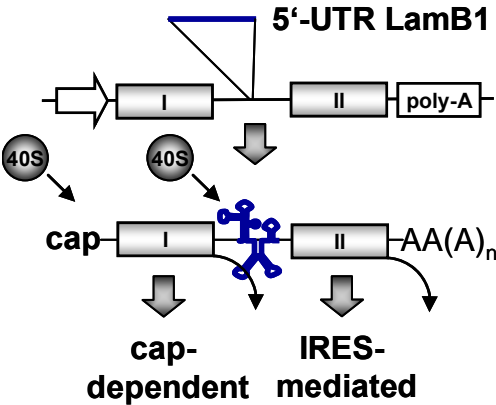


Figure 17 Translation of p β Gal/Lam/CAT reporters (Figure was kindly provided by Michaela Petz). (I) The β -Gal reporter is translated in a cap-dependent manner, whereas (II) the CAT reporter is produced in an IRES-mediated fashion.

5.4 Transient transfection

Cells were seeded onto collagen-coated 6-well plates. Respective cell numbers were seeded to reach a confluency of 70% after 24 hours (Table 1). For each transfection, 1 µg DNA (pβGal/Lam/CAT vector) were resuspended with 6 µl Plus reagent in 100 µl DMEM (Invitrogen, Carlsbad, USA). In a second tube, 4 µl Lipofectamine was resuspended in 100µl DMEM (Invitrogen, Carlsbad, USA). The two solutions were mixed after 15 minutes incubation at room temperature and incubated for another 15 minutes at room temperature. Cells were washed in PBS and then 0,8 ml DMEM as well as 0,2 ml transfection mix were drop-wise added to the cells. The medium was changed to full RPMI after 3 hours of incubation and, if not otherwise indicated, were cells cultured as described in 5.2. Cell extracts were prepared after 48 hours of transfection (see 5.5).

Table 1 Cell numbers seeded for transfection.

Cell Number/ 6-well	Cells
3×10^5	MIM-S35 and -C40
$3,5 \times 10^5$	MIM-R and -R-dnP
4×10^5	MIM-RT and -CT
$4,5 \times 10^5$	MIM-RT-dnP and -ST

5.5 Preparation of cell extracts

For RNA generation:

Cells were kept on ice during the whole procedure. 10 µl/ml β-mercaptoethanol was added to lysis buffer RLT (provided by RNeasy Mini Kit, Quiagen, Hilden, Germany). Cells were washed with cold PBS. 350 µl lysis buffer was added per 6-well and cells were incubated for 5 minutes. Cells were scraped, transferred into a tube and snap frozen. Lysates were stored at -20°C and for long-term storage at -80°C.

For β-Gal assay and CAT ELISA:

Cells were kept on ice during the whole procedure. Lysis buffer was prepared from CAT ELISA Kit as recommended by the manufacturer (Roche, Mannheim, Germany). Cells were washed with cold PBS, 500 µl lysis buffer was added per 6-well and incubated for 30 minutes. Cells were scraped, transferred into a tube and snap frozen. Lysates were stored at -20°C and for long-term storage at -80°C.

For Western blot:

Cells were kept on ice during the whole procedure. Phosphatase inhibitors consisting of 2 μ l 500 mM NaF, 2 μ l 5 mg/ml Leupeptin, 2 μ l 5 mg/ml Aprotinin, 1 μ l 1 M Na_3VO_4 and 10 μ l 100 mM PMSF in 100% ethanol were added to 1 ml RIPA lysis buffer. Cells were washed twice with cold PBS. Lysis buffer was added (200 μ l/10 cm plate, 100 μ l/6 cm plate and 80 μ l/6-well) and incubated for 10 minutes. Cells were scraped, transferred into a tube and snap frozen. Lysates were stored at -20°C .

Buffers and solutions:

- RIPA buffer:
 - 50 mM Tris pH 7,5
 - 150 mM NaCl
 - 1 mM β -Glycoperphosphate
 - 0,5% DOC
 - 1% NP-40

5.6 RNA isolation

To isolate total RNA the RNeasy Mini Quiagen Kit was used (Quiagen, Hilden, Germany). Prepared cell lysates (see 5.5) were passed 30 times through a 20 gouche needle. 350 μ l 70% ethanol (RNase free) was added, mixed by pipetting and transferred onto spin column. After 1 minute centrifugation at 20800 g, the supernatant was removed, 700 μ l buffer RW1 was added and centrifuged again. The supernatant was removed, 500 μ l buffer RPE were added and the column was again centrifuged. After removing the supernatant, 500 μ l buffer RPE were added and the column was centrifuged 2 minutes at 20800 g. Supernatant was removed and the column was centrifuged again for 2 minutes at 20800 g. To elute RNA the spin column was placed into a new RNase free tube and 30 μ l RNase free water was pipetted at the center of the column. After 5 minutes incubation, the column was centrifuged 1 minute at 20800 g. RNA was stored at -20°C or at -80°C for long-term.

5.7 Reverse transcription (RT)

To abrogate secondary RNA structures, 2 μ l wipeout buffer (Quiagen, Hilden, Germany), 5 μ l RNA sample and 7 μ l ddH₂O were mixed and incubated for 2 minutes at 42°C . The mix was immediately put on ice, 1 μ l primer mix, 4 μ l RT buffer and 1 μ l reverse transcriptase were

added and incubated for 30 minutes at 42°C (Quiagen, Hilden, Germany). To inactivate the reverse transcriptase, the mix was incubated 3 minutes at 95°C. cDNA was stored at -20°C.

5.8 Quantitative polymerase chain reaction (qPCR)

In a Fast Reaction Tube (Applied Biosystems, CA, USA), 3 µl cDNA (1:100 diluted in ddH₂O), 2 µl primer mix (4 µM stock of forward and reverse primer in ddH₂O) and 5 µl Fast SYBR green (Applied Biosystems, CA, USA) were mixed. Duplicates for RhoA and β-Gal were measured by the 7500 Fast Real Time PCR System (Applied Biosystems, CA, USA). Conditions for qPCR, see Table 2; Primer sequences, see Table 3.

Table 2 qPCR conditions.

Step	1	2	3
Function	Enzyme activation	Denaturation	Anneal/Extend
Repeat	1		40
Temp [°C]	95	95	60
Time [sec]	20	3	30

Table 3 Primer sequences.

Primer	Forward	Reverse
β-Gal	ACTATCCCGACCGCCTTACT	CTGTAGCGCTGATGTTGAA
RhoA	GGAAGAAACTGGTGATTGTTGGTG	TCGTGGTTGGCTTCTAAATACTGG

5.9 β-Galactosidase assay

Cell lysates (see 5.5) were centrifuged 10 minutes at 16100 g and 4°C. For each sample, 4 µl 100 x Mg solution, 88 µl o-nitrophenyl-β-d-galactopyranoside (ONPG) solution, 268 µl 0,1 M sodium phosphate solution and 20-30 µl cell lysate were mixed. Reaction mix without lysate was used as blank. The reaction mix was incubated for at least 30 minutes at 37°C until a faint yellow color had developed. Samples were measured in triplicates (each 100µl) at 405 nm.

Buffers and solutions (stored at 4°C):

- 100 x Mg solution:
 - 0,1 M MgCl₂
 - 4,5 M β-Mercaptoethanol
- 0,1 M sodiumphosphate solution pH7,5:
 - 16,4 ml 0,5 M Na₂HPO₄
 - 9 ml 0,2 M NaH₂PO₄
 - 74,6 ml ddH₂O
- ONPG:

4 mg/ml in 0,1 M sodiumphosphate pH 7,5

5.10 CAT ELISA

Procedure was performed with the CAT ELISA kit (Roche, Mannheim, Germany). Cell lysates (see 5.9) were applied in duplicates. 200 µl cell lysate was pipetted into each well. The plate was covered with foil and incubated for 1 hour at 37°C. After three times washing with 200 µl washing buffer 200 µl 2 µg/ml anti-CAT-DIG in sample buffer was added per well. The plate was covered with foil and incubated for 1 hour at 37°C. The ELISA was washed three times with 200 µl washing buffer, 200 µl 150 mU/ml anti-DIG-POD in sample buffer was added per well. The plate was covered with foil and incubated for 1 hour at 37°C. The ELISA was washed three times with 200 µl washing buffer, 200 µl POD substrate was added per well and incubated 10-40 minutes at room temperature until the appropriate development of green color. Each well was resuspended to ensure homogeneous distribution of the reaction product. The OD was measured at 405 nm.

5.11 Calculations for bicistronic assays

qPCR for β-Gal:

First the average of the two measured Ct values was calculated. Then the mean-RhoA value was subtracted from corresponding mean-β-Gal value to calculate ΔCt. Relative expression E was calculated by the formula $E = 2^{-\Delta Ct}$.

β-Gal assay:

The average of the three measured values was calculated and the mean blank was subtracted from mean-sample value. Normalization to the mRNA levels was used in assays that interfered with translation (assays using PI3K and MEK1/2 inhibitors). Therefore, the calculated β-Gal values were divided through the corresponding E values of qPCR.

CAT ELISA:

The average of the two measurements was calculated. Normalization to the mRNA levels was used in assays that interfered with translation (assays using PI3K and MEK1/2 inhibitors). Therefore the calculated CAT values were divided through the corresponding E values of qPCR. For normalization of the other assays, the calculated CAT values were divided through the corresponding β-Gal-values.

End-analysis and statistics:

Bicistronic assays were carried out at least in triplicates and results correspond to the average of at least three independent experiments. Statistical significance was calculated by paired Student's t-test, p-values (p) <0,05 (*), <0,01 (**), and <0,005 (***) indicate statistical significant differences.

5.12 Bradford assay and Western blot sample preparation

Cell lysates (see 5.5) were centrifuged 5 minutes at 16100 g and 4°C. The supernatants were transferred in a new tube and 1:5-1:20 dilutions in ddH₂O were prepared to determine protein concentrations. Bradford reagent (Protein assay, BioRad, Munich, Germany) was diluted 1:5 in ddH₂O and 400 µl of the fresh prepared Bradford solution were mixed with 10 µl of sample or BSA standards. After vortexing and incubation for 5 minutes at room temperature, 3 x 100 µl of Bradford mix were transferred in a 96 well plate and measured at 620 nm. A BSA standard curve was calculated and protein sample concentration was determined. 30 µg protein were diluted with PBS to a total volume of 10 µl and 10 µl 2xSDS sample buffer was added. Prepared samples were used for Western blotting and stored at -20°C.

Buffers and solutions:

- BSA standards:

BSA dilutions in ddH₂O were prepared with following concentrations: BSA [mg/ml]
0,1; 0,2; 0,4; 0,6; 1,8; 1,0; 1,2 and stored at -20°C

- 2 x SDS sample buffer:

1 ml Tris/HCl pH 6,8

2,5 ml 20% SDS

0,5 ml β-Mercaptoethanol

4 ml 50% glycine

0,5 ml 1M DTT

1,5 ml ddH₂O

0,2% bromphenole blue

5.13 Western blot

SDS polyacrylamide gel electrophoresis (SDS-PAGE):

The gel apparatus with 0,75 mm spacer was assembled. To prepare two 10% separation gels 4,45 ml 30% PAA/1% PDA; 2,5 ml 2 M Tris pH 8,8; 6,2 ml ddH₂O; 45 µl 10% APS and 7,5 µl TEMED were mixed and immediately filled into gel apparatus until the gel reached 1 cm below the upper edge. Gels were overlaid with isopropanol and allowed to polymerize. Isopropanol was removed, gels were washed three times with ddH₂O and the water was removed with a piece of whatman paper. Stacking gels were prepared by mixing 0,5 ml 30% PAA/1% PDA; 0,5 ml 1 M Tris pH 6,8; 3 ml ddH₂O; 20 µl 10% APS and 4 µl TEMED and filled immediately into the gel apparatus. The comb was inserted and the gels were left for polymerization. Gels were placed into gel electrophoresis chambers and filled up with electrophoresis buffer. The combs were removed and slots were rinsed with electrophoresis buffer. Prepared cell extract samples (see 5.12) were heated for 2 minutes at 95°C, cooled down on ice and spun down. Samples (18 µl for comb with 10 slots and 10 µl for comb with 15 slots) or 5µl prestained protein ladder (Fermentas, Maryland, USA) were loaded. A current of 15 mA/gel was applied for 1-2 hours. Electrophoresis buffer was reused several times.

Blot:

One nitrocellulose membrane, three 3 mm Whatman papers and two pads were wetted in blotting buffer for each gel. Blotting sandwich was assembled according to Table 4 and air bubbles were removed. Then the blotting sandwich was placed into the blotting chamber with stir bone and ice for cooling. The chamber was filled up with blotting buffer and a constant voltage of 100 V was applied for 1 hour. The blotting buffer was reused several times.

Table 4 Schema for blotting sandwich.

1.	Black plastic (minus pole)
2.	Pad
3.	Whatman paper
4.	Gel
5.	Nitrocellulose membrane
6.	2x Whatman papers
7.	Pad
8.	White plastic (plus pole)

Membrane developing and detection:

The membrane was washed with ddH₂O and stained for 1-2 minutes with Ponceau S. The membrane was washed with ddH₂O until bands were visible. After imaging, the membrane

was cut into appropriate pieces. Then the Ponceau staining was completely washed out and the membrane was blocked in 5% BSA in TBST (for LamB1 antibody in 1% Milk in TBST) for 1 hour at room temperature with shaking. The 1st antibody was diluted in TBST (see Table 5), applied to the membrane and incubated over night at 4°C with shaking. The 1st antibody solution was saved and stored at -20°C for reuse. The membrane was washed 3 times for 15 minutes with TBST and incubated with 2nd antibody diluted in TBST (see Table 6) for 1 hour at room temperature with shaking. Then the membrane was washed three times for 10 minutes with TBST and put on a glass plate where it was incubated 2 minutes with freshly prepared ECL- H₂O₂ solution. Per ml Luminol/ Coomarcic solution, 3 µl 3% H₂O₂ were added and vortexed. After dripping the membrane on a paper towel, it was put into a cassette and developed in a darkroom with a hyperfilm (Amersham HyperfilmTM ECL, GE Healthcare Limited, Buckinghamshire, UK).

Table 5 1st antibodies.

Antibody	Company	Dilution	Reactivity	Source	Size [kDa]
Actin	Sigma	1 : 2000	wide range	r	42
Phospho-Akt	Cell Signaling	1 : 1000	h, m, rat, c	r	60
Akt	BD Transduction Lab	1 : 1000	h, m, rat, dog	m	59
Phospho-Erk	Cell Signaling	1 : 1000	h, m, rat, hm, c	r	42, 44
Erk	Cell Signaling	1 : 1000	h, m, rat, hm	r	42, 44
La	Cell Signaling	1 : 2000	h, m, rat, mk	r	50
LamB1	NeoMarker	1 : 1000	h, m, pig, hm	rat	210
Nucleoporin	BD Transduction Lab	1 : 1000	m, rat, c	m	62
Tubulin- α	Sigma	1 : 1000	h, m, rat, b, c	m	50

b = bovine, c = chicken, dog = dog, hm = hamster, h = human, mk = monkey, m = mouse, pig = pig, r = rabbit, rat = rat

Table 6 2nd antibodies.

Conjugate	Company	Dilution	Reactivity	Source
Peroxidase	Vector Laboratories	1 : 10000	Mouse IgG	Horse
Peroxidase	Vector Laboratories	1 : 10000	Rabbit IgG	Goat
Peroxidase	Santa Cruz	1 : 10000	Rat IgG	Goat

Stripping:

7 µl β -Mercaptoethanol were added to 1 ml stripping buffer. The buffer was applied to the membrane and incubated for 30 minutes at 50°C to remove attached antibodies. The membrane was washed with ddH₂O until it was inodorous, followed by three times washing for 10 minutes with TBST. Then the membrane was blocked for one hour and antibodies were applied.

Buffers and solutions:

- 30% Acrylamide/ Bisacrylamide solution:
292,1 g Acrylamide
7,8 g bisacrylamide
Fill up with ddH₂O to 1 l, sterile filtrate, and store at 4°C with light protection
- 10 x Tris/ glycine:
25 mM Tris
192 mM Glycine
- Electrophoresis buffer:
100 ml 10 x Tris/glycine
5 ml 20% SDS
Adjust with ddH₂O to 1 l
- Blotting buffer:
100 ml 10 x Tris/glycine
150 ml methanol
1 ml 20% SDS
Adjust with ddH₂O to 1 l
- 10 x TBS (low salt Tris-buffered saline):
200 mM Tris
1,5 M NaCl
Adjust pH to 7,5
- TBST:
10 ml 10% Tween in 1l 1xTBS (final 0,1% Tween)
- Ponceau S:
0,2% Ponceau in 3% trischloroacetic acid (TCA)
- Stripping buffer:
20 mM Tris/HCl pH 6,8
2% SDS
- Luminol/ Coomarcic solution:
200 ml 0,1M Tris pH 8,8
500 µl p-Coumaric acid (stock: 340 mg in 26 ml DMSO)
1 ml Luminol (stock: 2,26 g in 51 ml DMSO)

5.14 Reverse transcriptase (RT)-PCR

cDNAs were diluted in ddH₂O to adjust RhoA amplification products to each other. For RT-PCR, 10 µl cDNA dilution, 15 µl primer mix (4 µM stock of forward and reverse primer in ddH₂O; primer sequences see Table 7) and 1 Ready-To-Go bead (Amersham, Uppsala, Sweden) were mixed in a PCR tube. The following PCR program was used: 2 cycles 63°C, 2 cycles 61°C, 32 cycles 59°C. Amplified PCR products were analyzed by agarose gel electrophoresis.

Table 7 Primer sequences.

Primer	Forward	Reverse	Amplicon [bp]
PDGF-A	GGCTTGCCTGCTGCTCCTCG	CTCCACTTTGGCCACCTTGAC	456
PDGF-R α	CAGACTTCGGAAGAGAGTGCCATC	CAGTACAAGTTGGCGCGTGTGG	468
PDGF-B	TGCTGAGCGACCACTCCATC	GATTCTCACCGTCCGAATGG	550
PDGF-R β	CCTGAACGTGGTCAACCTGCT	GGCATTGTAGAACTGGTTCGT	765
RhoA	GGAAGAACTGGTGATTGTTGGTG	TCGTGGTTGGCTTCTAAATACTGG	721

5.15 Agarose gel electrophoresis

1% agarose was dissolved in 1 x TAE by heating. Ethidium Bromide was added at a ratio of 1: 10000 after the solution was cooled down. The gel was poured into the apparatus and left for polymerization. 5 x loading buffer was added to PCR products (form 5.14.) and 10-15 µl sample or 4 µl 100 bp Plus DNA Gene Ruler (Fermentas, Maryland, USA) was loaded. A voltage of 100 V was applied to the gel for at least 30 minutes. Pictures were taken with a gel imaging software.

Buffers and solutions:

- 50 x TAE:
 - 242 g Tris
 - 57,1 ml glacial acetic acid
 - 100 ml 0,5 M EDTA pH 8
 - Adjust with ddH₂O to 1 l and sterile filtrate
- 5 x Loading buffer:
 - 60 mM Tris/HCl pH 7,5
 - 40% sucrose (w/v)
 - 0,2% bromphenole blue
 - Store at 4°C

6 RESULTS

6.1 LamB1 IRES translation is controlled by MAPK and PI3K pathway

Constitutive activation of Ras and TGF- β signaling induces EMT in murine hepatocytes [42]. Recently it was shown that LamB1 IRES translation as well as MAPK and PI3K signaling is elevated in these EMT-transformed cells [42, 100]. Since these two pathways are known to be important for the regulation of translation, we addressed the question whether they are responsible for LamB1 IRES activity [79]. We therefore employed several hepatic cell lines for these studies. MIM-R cells express constitutive active Ha-Ras whereas MIM-S35 and MIM -C40 either expresses a Ras mutant selectively activating MAPK or PI3K pathway in response to cognate signals, respectively [42]. Epithelial MIM-S35, -C40 -and -R as well as their corresponding EMT-transformed cells (MIM-ST, MIM -CT and MIM -RT) were transfected with the bicistronic vector p β Gal/Lam/CAT and analyzed for LamB1 IRES activity (Figure 18). Furthermore, we studied LamB1 IRES translation at the initial steps of EMT. Hence, we treated MIM-S35, MIM -C40 and MIM-R cells after bicistronic vector transfection for 24 hours with TGF- β . Untreated epithelial cell lines showed almost same levels of relative CAT activities, thus LamB1 IRES activities. After 24 hours TGF- β treatment, LamB1 IRES activity was not significantly increased. Highest IRES activity was observed in EMT-transformed cells, which corroborates previously observed findings [100]. Notably, levels in MIM-ST and MIM -RT cells were higher than in MIM-CT. Although 24 hours TGF- β treatment did not increase LamB1 IRES translation, these results show that TGF- β -mediated EMT-transformation leads to elevated LamB1 IRES activity. Furthermore, the data indicate that the PI3K as well as the MAPK pathway influence LamB1 IRES translation and that the latter one could be more important upon EMT.

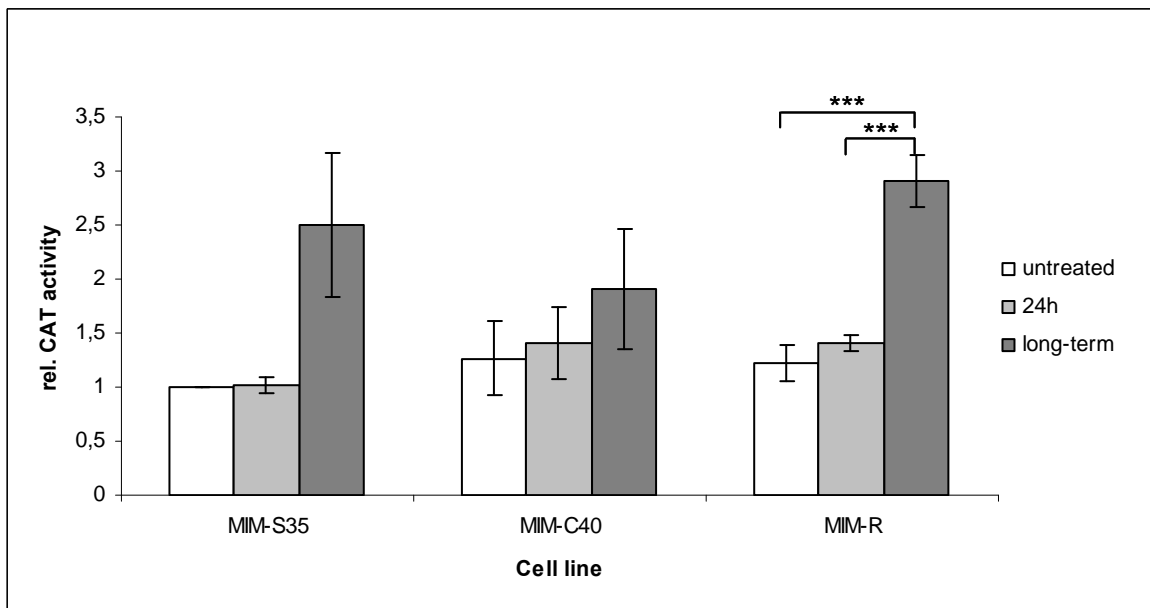


Figure 18 LamB1 IRES translation is increased upon EMT and is affected by the PI3K and MAPK pathway. Different hepatocyte cell lines including MIM-S35 and MIM -C40 which selectively activate MAPK or PI3K pathway, respectively and MIM-R which expresses a constitutive active Ras were transfected with pβGal/Lam/CAT and treated 24 hours or long-term with TGF-β. LamB1 IRES activity was assessed by relative CAT activity (CAT to β-Gal ratio). *** p<0,005

Since we observed that LamB1 IRES is affected by PI3K and MAPK pathway, we analyzed the downstream targets AKT and ERK, respectively, as well as LamB1 protein levels in cell lines that were used for the bicistronic assay (Figure 18). Recently, it was observed that La regulates the LamB1 IRES [101]. Furthermore, it has been reported that the protein expression of La is regulated by AKT [129]. We therefore determined whether La protein levels differ in the cell lines under investigation. Protein lysates of above described MIM-S35, MIM-C40 -and MIM -R cells, as well as MIM-ST, MIM -CT and MIM -RT cells were subjected to Western blot analysis (Figure 19). Comparing untreated epithelial cells, MIM-C40 showed highest p-AKT levels. Moreover, untreated MIM-S35 and MIM -R had similar levels of p-ERK, which were higher than in MIM-C40. In line with previous studies, AKT activity was low after 24 hours TGF-β treatment and EMT transformation lead to a strong increase (manuscript in preparation). 24 hours TGF-β treatment did not influence p-ERK levels in MIM-S35 and MIM-R but induced a slight elevation in MIM-C40 cells. Long-term treated cells showed the highest ERK activation. Interestingly, ERK activity decreased from MIM-ST to MIM -RT to MIM-CT. La levels were not different in investigated cells and

Lamb1 expression raised during course of TGF- β treatment. Notably, lowest Lamb1 levels were in untreated MIM-C40 cells, which elevated to a high degree after 24 hours TGF- β treatment. However, MIM-CT had lower Lamb1 levels than MIM-ST and MIM-RT. On the one hand results confirm selective activation of PI3K and MAPK pathway in MIM-C40 or MIM-S35, respectively. On the other hand they show that during EMT transformation the activation of these two pathways correlates with increased Lamb1 expression. This points to a regulative role of PI3K and MAPK pathway in Lamb1 IRES translation. In line with results of the bicistronic assay (Figure 18), these data suggest that MAPK pathway is more important for Lamb1 expression.

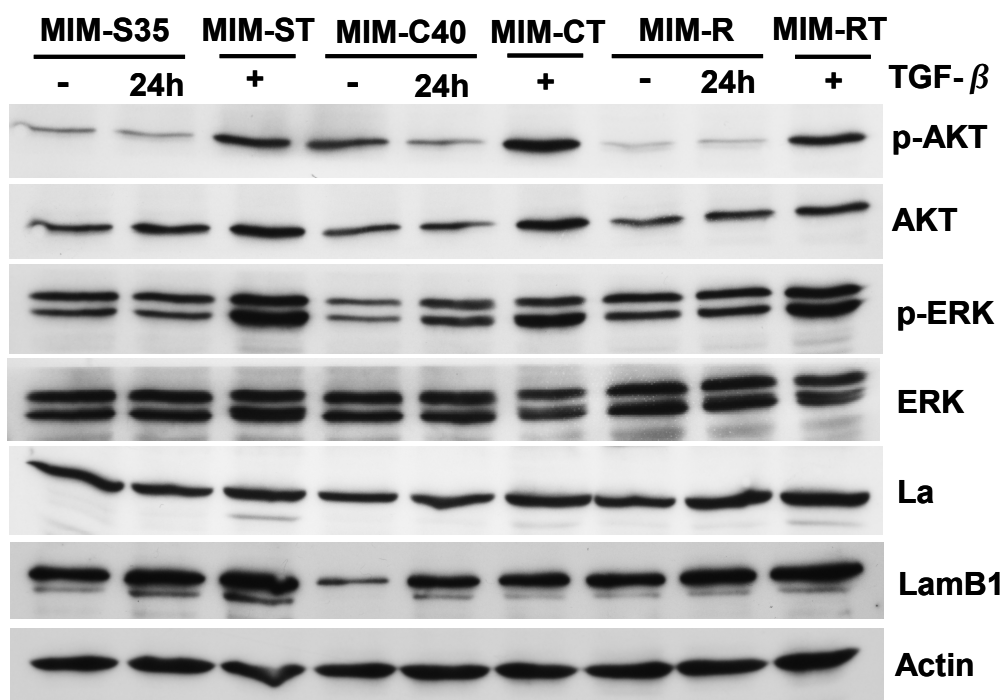


Figure 19 Lamb1 expression correlates with activation of PI3K and MAPK pathway. Different MIM hepatocytes (MIM-S35 and MIM-C40 selectively activating MAPK or PI3K pathway, respectively, and MIM-R expressing constitutive active Ras) were treated 24 hours or long-term with TGF- β . AKT and ERK activation as well as La and Lamb1 levels were analyzed by Western blotting.

6.2 MAPK pathway predominantly regulates Lamb1 expression in epithelial hepatocytes

Investigation of the hepatic cell lines MIM-S35, MIM-C40 and MIM-R revealed that Lamb1 IRES translation is controlled by PI3K and MAPK pathway. We further evaluated the role of these pathways on Lamb1 IRES expression by applying pharmacological inhibitors against

PI3K and MAPK pathway. Epithelial MIM-R and mesenchymal MIM-RT were transfected with the bicistronic vector p β Gal/Lam/CAT, treated with PI3K or MEK1/2 inhibitor and analyzed for LamB1 IRES activity (Figure 20). Both inhibitors had a significant effect on LamB1 IRES translation in MIM-R cells (Figure 20A). Compared to the DMSO treated control, LamB1 IRES translation was reduced to 50% activity upon inhibition of PI3K pathway and was even more decreased to 35% residual activity when interfering with MAPK pathway. In EMT-transformed MIM-RT cells, the inhibitors had only marginal effects on LamB1 IRES translation (Figure 20B). Upon PI3K pathway inhibition, LamB1 IRES activity was almost as high as in the DMSO treated control and MAPK inhibition lead to 40% reduction of LamB1 IRES translation. Taken together, the results support the observations that PI3K and MAPK pathway regulate LamB1 IRES translation and that the latter one might have a greater impact. Interestingly, PI3K and MAPK pathway did not inhibit LamB1 IRES activities to the same extend in MIM-R and MIM-RT cells. These results suggest that the PI3K and especially the MAPK signaling control LamB1 IRES translation in MIM-R hepatocytes and that in EMT-transformed MIM-RT cells LamB1 IRES activity is influenced by additional mechanisms.

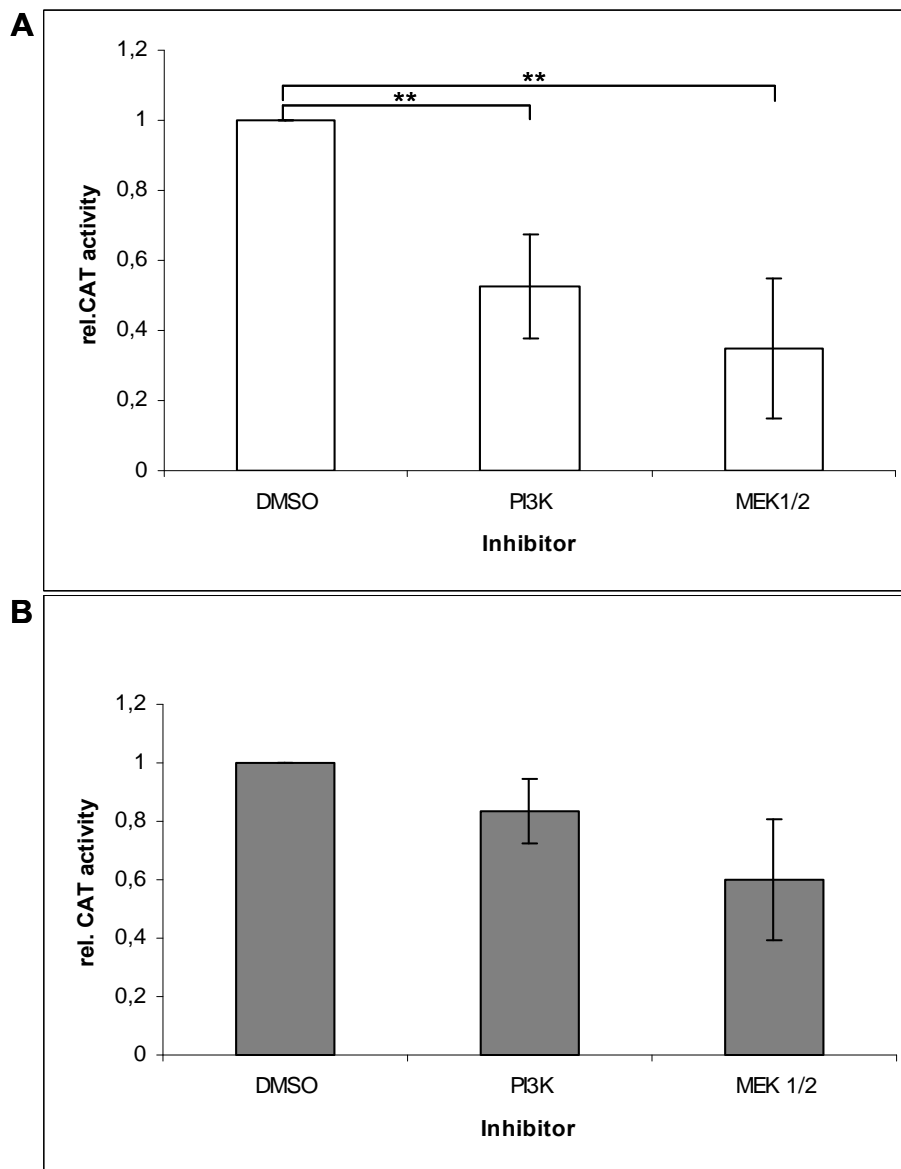


Figure 20 Inhibition of PI3K and MAPK pathway decreases Lamb1 IRES translation to a different extend in MIM-R and MIM-RT cells. (A) MIM-R and (B) MIM-RT were transfected with pβGal/Lam/CAT and treated for 24 hours with inhibitors against PI3K or MEK1/2. Same amounts of DMSO served as vehicle control. Lamb1 IRES activity was assessed by relative CAT activity (CAT values were normalized to mRNA levels). ** p<0,01

We further addressed the question whether specific inhibition of PI3K or MAPK pathway has an impact on the signaling required for Lamb1 translation. MIM-R and MIM-RT cells were therefore treated with PI3K or MEK1/2 inhibitors and then analyzed by Western blotting (Figure 21). In both cell lines, specific inhibition of PI3K resulted in decreased p-AKT levels and MEK1/2 inhibition to reduced p-ERK levels. Interestingly, the PI3K inhibitor caused MAPK pathway activation and MEK1/2 inhibitor PI3K pathway activation in MIM-RT cells.

La expression was similar in the investigated cells, nevertheless, in MEK1/2 treated MIM-R there was a slight decrease. Notably, besides the specific upper La band one lower band appeared in all cells besides MEK1/2 inhibited cells. Consistent with previous studies, MIM-RT control cells displayed higher LamB1 levels than MIM-R control cells [100]. PI3K inhibitor treated MIM-R and MIM-RT cells showed no difference in LamB1 levels compared to their controls. Upon MEK1/2 inhibition, the LamB1 level did not change in MIM-RT cells, however levels were reduced in MIM-R cells. Results show that interference with MEK1/2 in MIM-R cells is sufficient to impair LamB1 expression, indicating that MAPK pathway is important for LamB1 translation in epithelial hepatocytes. In addition, observations in MIM-RT propose that these cells can bypass inhibition of PI3K or MAPK pathway by activating (an) alternative pathway(s). Hence, possibly either both pathways influence LamB1 translation or none of them is essential for the enhancement of LamB1 translation in EMT-transformed cells.

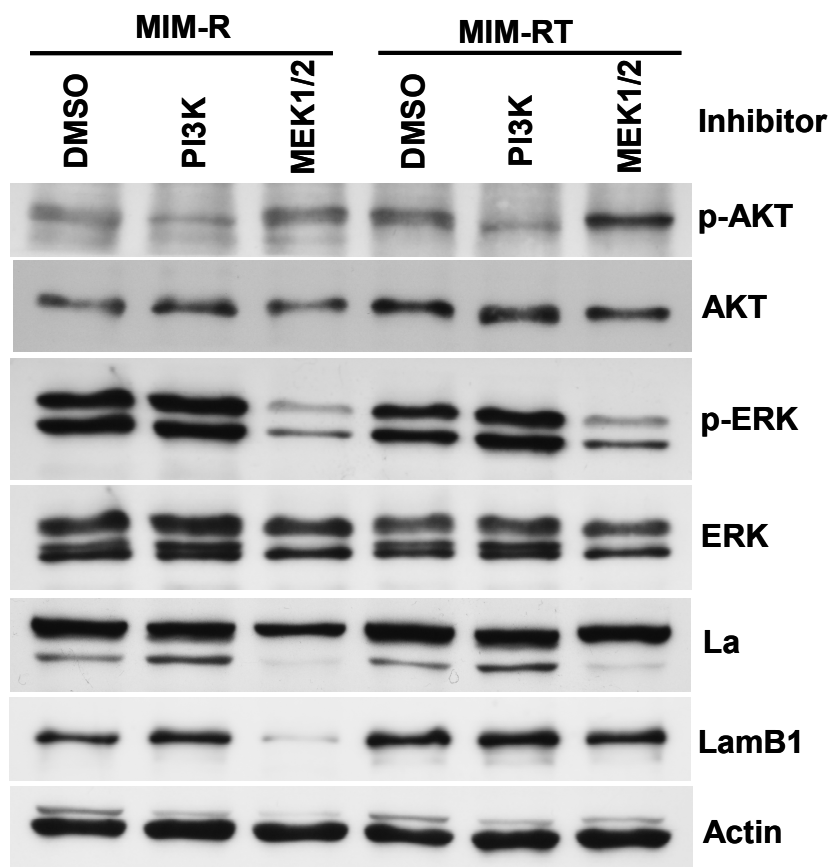


Figure 21 LamB1 expression is reduced upon MEK1/2 inhibition in MIM-R and is not decreased in MIM-RT upon inhibition of MEK1/2 or PI3K. MIM-R and MIM-RT cells were treated 24 hours with PI3K or MEK1/2 inhibitor and same amounts of DMSO served as vehicle control. Protein lysates were analyzed by Western blot for AKT and ERK activation as well as for La and LamB1 levels.

6.3 PI3K and MAPK pathway regulate LamB1 expression in mesenchymal hepatocytes

Since inhibitor studies revealed that MIM-RT cells are insensitive to inhibition of either PI3K or MAPK pathway, we addressed the question whether MIM-RT cells are sensitive to the combined inhibition of PI3K and MAPK pathway. Therefore, EMT-transformed MIM-RT cells were transfected with the bicistronic vector p β Gal/Lam/CAT, treated with PI3K together with MEK1/2 inhibitor and analyzed for LamB1 IRES activity (Figure 22A). Combined inhibition had a significant effect on LamB1 IRES translation in MIM-RT cells. Compared to the DMSO treated control, LamB1 IRES translation was reduced to 35% residual activity when interfering with PI3K and MAPK pathway. These results together with data of single inhibitions (Figure 20B) indicate that PI3K or MAPK pathway alone are able to control LamB1 IRES translation and that the combined inhibition is needed to decrease LamB1 IRES activity in EMT-transformed cells.

We further investigated the effect of combined inhibition of PI3K and MAPK pathway on the signaling required for LamB1 translation. MIM-RT cells were treated with PI3K and MEK1/2 inhibitor and analyzed by Western blotting (Figure 22B). Specific inhibition of PI3K and MEK1/2 resulted in decreased p-AKT and p-ERK levels. La expression was similar in the investigated cells. Although inhibition of either PI3K or MEK1/2 did not change LamB1 protein levels (Figure 21), combined inhibition lead to reduced LamB1 expression in MIM-RT cells. Taken together, these data show that PI3K as well as MAPK pathway regulate LamB1 translation in EMT-transformed cells.

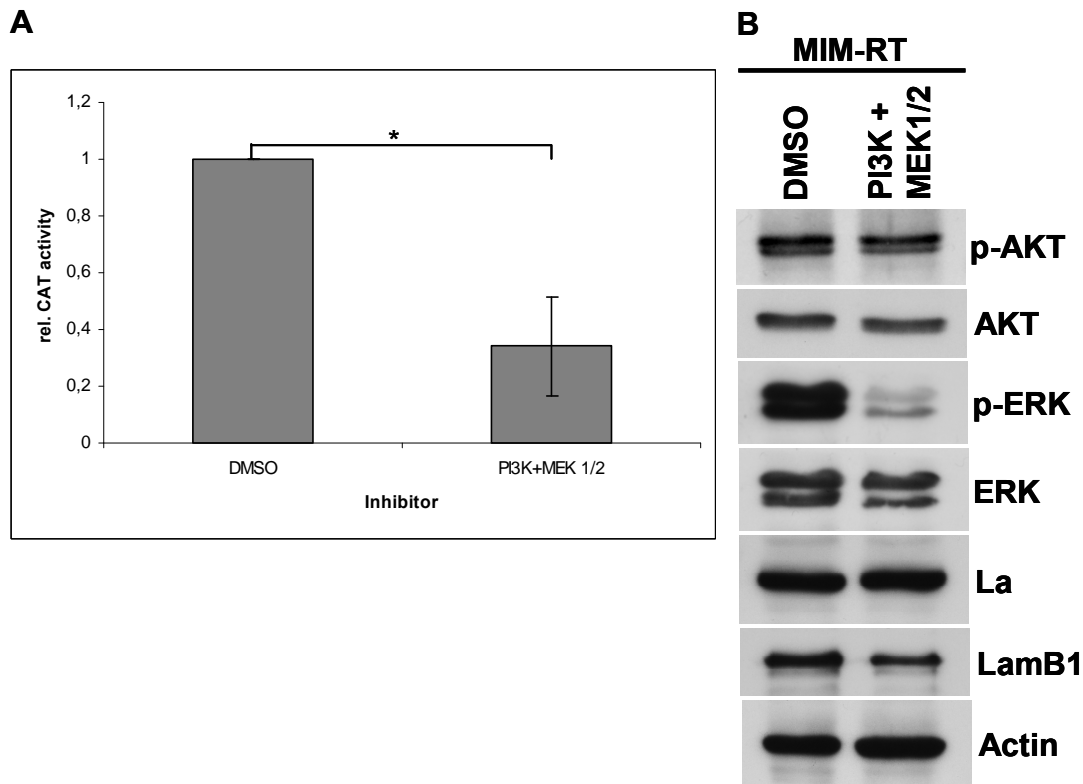


Figure 22 Inhibition of PI3K together with MAPK pathway decreases LamB1 IRES translation and LamB1 expression in MIM-RT cells. (A) MIM-RT cells were transfected with p β Gal/Lam/CAT and treated for 24 hours with inhibitors against PI3K and MEK1/2. Same amounts of DMSO served as vehicle control. LamB1 IRES activity was assessed by relative CAT activity (CAT values were normalized to mRNA levels). * $p < 0,05$ (B) MIM-RT cells were treated 24 hours with PI3K and MEK1/2 inhibitor and same amounts of DMSO served as vehicle control. Protein lysates were analyzed by Western blot for AKT and ERK activation as well as for La and LamB1 levels.

6.4 EMT-transformed cells activate PDGF signaling

Moreover, we aimed to identify additional signaling pathways, besides TGF- β signaling, that activate AKT as well as ERK signaling upon EMT, thereby controlling LamB1 IRES translation. We decided to stimulate cells for 30 minutes with different growth factors to evaluate immediate response and 2 hours to analyze late signaling events. FCS, TGF- α , insulin and PDGF were used for stimulation since these are known to activate PI3K and MAPK pathway [67, 68, 70, 135-139]. MIM-R and MIM-RT cells were serum starved for 24 hours, stimulated for 30 minutes or 2 hours with FCS, TGF- α , insulin or PDGF and analyzed by Western blotting for LamB1 levels, AKT and ERK activation (Figure 23). TGF- α and FCS activated ERK after 30 minutes but did not influence AKT activity in both cell lines. Insulin

increased p-AKT and p-ERK levels in MIM-R and MIM-RT cells after 30 minutes. Interestingly, PDGF was able to activate AKT and ERK in MIM-RT but not in MIM-R cells after 30 minutes. All AKT and/ or ERK activations were downregulated after 2 hours stimulation and were most persistent in insulin- as well as TGF- α -treated cells. LamB1 expression was not influenced, except of a slight increase in MIM-RT after 2 hours PDGF-treatment. This experiment indicates that MIM-R and MIM-RT cells are capable for FCS, TGF- α and insulin stimulation, however, MIM-RT cells exclusively respond to the PDGF stimulus.

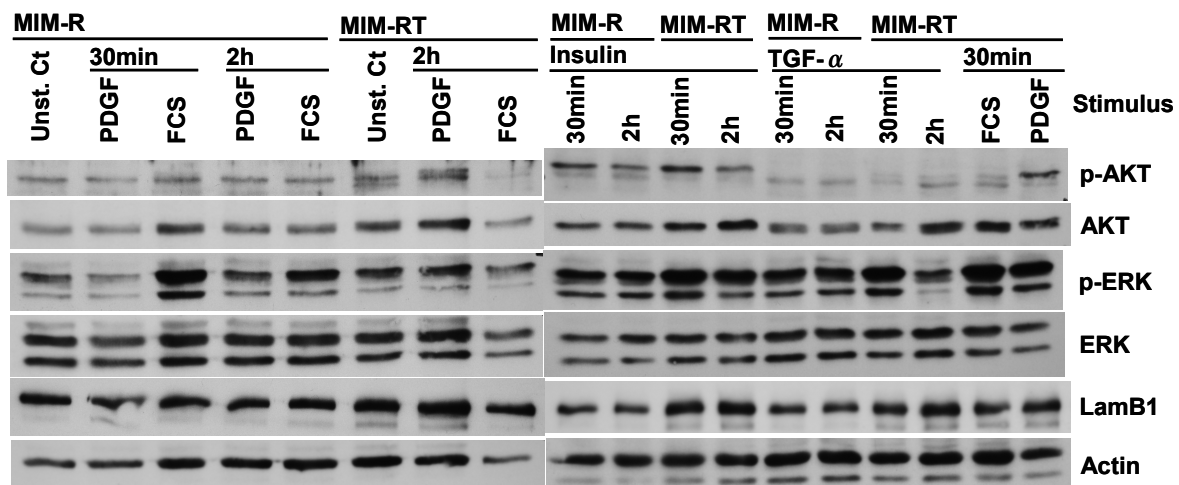


Figure 23 MIM-R and MIM-RT respond to FCS, TGF- α and insulin stimulation, but only MIM-RT to PDGF. MIM-R and MIM-RT were 24 hours serum starved and stimulated with FCS, TGF- α , insulin and PDGF for 30 minutes or 2 hours. Protein lysates were analyzed by Western blotting for AKT and ERK activation as well as for LamB1 levels.

It was recently reported that EMT leads to autocrine activation of PDGF signaling in murine hepatocytes (MIM-RT) [44]. As MIM-RT cells were sensitive to PDGF stimulation, which is in line with these results, we determined PDGF signaling in different hepatocytic MIM cells. MIM-R-dnP and MIM-RT-dnP cells that express the dominant negative PDGF-R α were employed for further studies [44]. PDGF-A, -B, -R α and -R β levels were analyzed by RT-PCR in epithelial MIM-S35, MIM-C40, MIM-R and MIM-R-dnP as well as in their corresponding EMT-transformed cells (MIM-ST, MIM-CT, MIM-RT and MIM-RT-dnP) (Figure 24). PDGF-A was expressed in all epithelial cells and levels increased in mesenchymal cells, except in MIM-RT-dnP. Similarly, PDGF-B, -R α and -R β levels were elevated in EMT-transformed cells compared to their epithelial cells. Notably, MIM-R-dnP and MIM-RT-dnP showed similar PDGF-R α levels due to the expression of dominant

negative PDGF-R α in these cell lines. The results suggest that not only MIM-RT but also all other EMT-transformed MIM cell lines exhibit enhanced PDGF signaling.

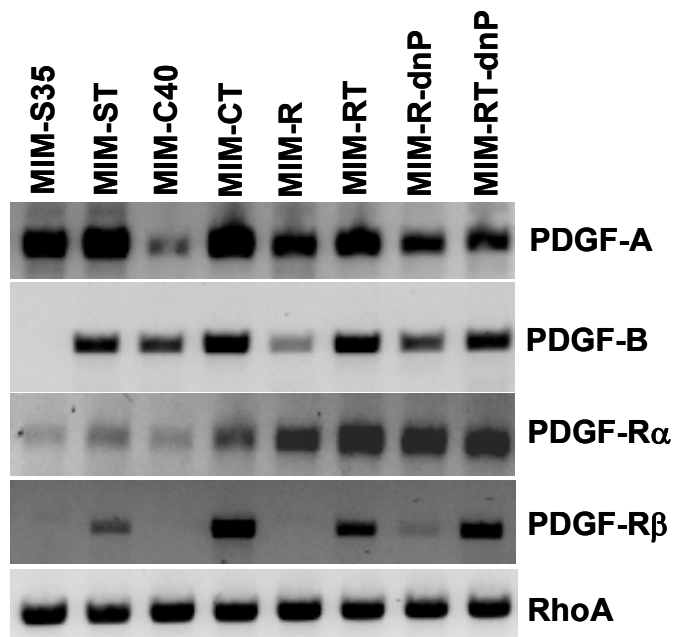


Figure 24 PDGF signaling is increased in EMT-transformed hepatocytes. Cell lines were analyzed for PDGF-A, -B, -R α and -R β expression by semi-quantitative RT-PCR.

6.5 PDGF controls cytoplasmic La accumulation and LamB1 IRES translation upon EMT

As mentioned in the introduction, cytoplasmic La localization is enhanced upon TGF- β -induced EMT [101]. Interestingly, it was reported that cytoplasmic La translocation is regulated by PDGF [129]. We therefore investigated the impact of PDGF on cytoplasmic La localization in our cell model as PDGF signaling is increased upon hepatocellular EMT. Michaela Petz treated MIM-R, MIM-RT, MIM-R-dnP and MIM-RT-dnP with 20 ng/ml PDGF for 24 hours, isolated cytoplasmic and nuclear fractions, which were subsequently subjected to Western blot analysis (Figure 25). Tubulin and nucleoporin were used as controls for cytoplasmic or nuclear fractions, respectively. Both EMT-transformed cells showed higher LamB1 levels and cytoplasmic La levels than their corresponding epithelial cells. More importantly, LamB1 and cytoplasmic La levels increased only in MIM-RT cells upon PDGF treatment. These results suggest that PDGF regulates cytoplasmic La accumulation and LamB1 expression in EMT-transformed cells. They furthermore indicate that there is probably an additional, PDGF-independent, pathway for cytoplasmic La localization and

LamB1 expression since MIM-RT-dnP cells also displayed higher LamB1 levels and cytoplasmic La compared to their epithelial cells.

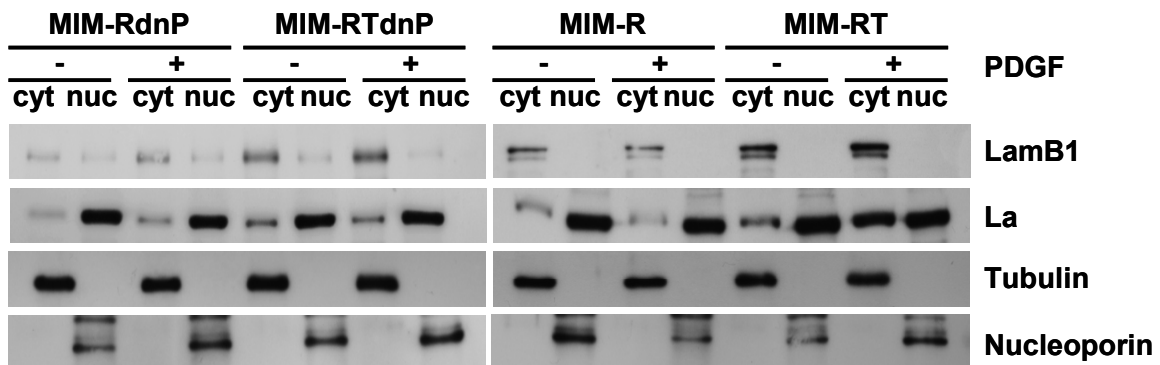


Figure 25 PDGF signaling controls LamB1 expression and cytoplasmic La accumulation in hepatocellular EMT. Michaela Petz treated MIM cells with 20 ng/ml PDGF for 24 hours and analyzed cytoplasmic and nuclear fractions by Western blotting. Tubulin and nucleoporin served as controls for cytoplasmic and nuclear fractions, respectively.

To evaluate the direct consequence of PDGF signaling on LamB1 IRES activity upon EMT, we transfected MIM-RT as well as MIM-RT-dnP with the bicistronic vector pβGal/Lam/CAT and treated the cells with PDGF (Figure 26). Additionally, a TGF-β-RI/II inhibitor was applied to prevent TGF-β-mediated autocrine PDGF signaling. As expected, untreated MIM-RT showed higher LamB1 IRES translation than MIM-RT-dnP. Inhibition of TGF-β signaling did not influence LamB1 IRES activity in untreated MIM-RT cells. Interestingly, PDGF stimulation resulted in increased LamB1 IRES translation only in MIM-RT treated with TGF-β-RI/II inhibitor. Together, these results propose that PDGF enhances LamB1 IRES activity by regulating cytoplasmic La translocation.

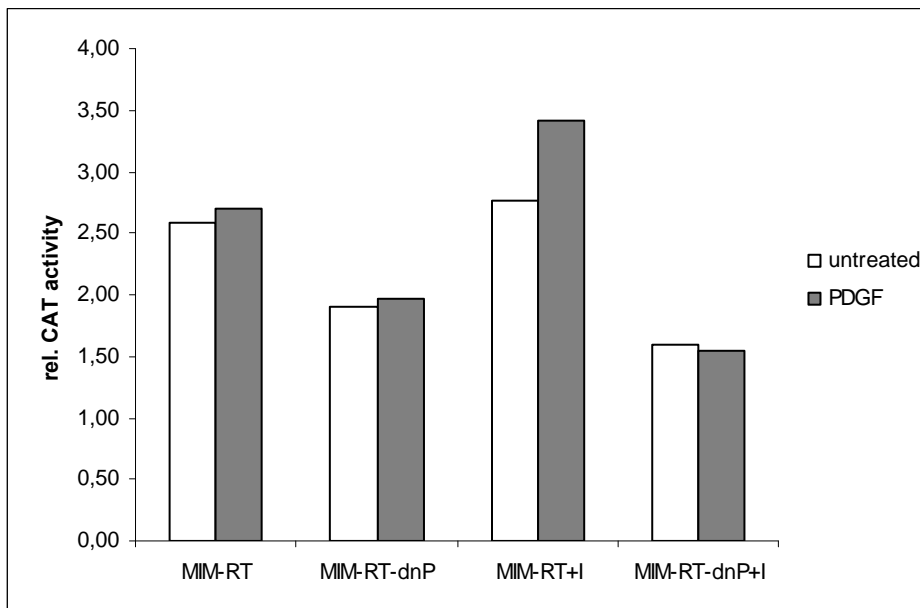


Figure 26 PDGF positively regulates Lamb1 IRES translation in EMT-transformed cells. MIM-RT and MIM-RT-dnP cells were transfected with pβGal/Lam/CAT and treated for 24 hours with PDGF and TGF-β-RI/II inhibitor (+I). Lamb1 IRES activity was assessed by relative CAT activity (CAT to β-Gal ratio). Please note that this assay was performed once and must be repeated.

6.6 Further investigation of PDGF downstream signaling

To further understand how Lamb1 IRES translation is regulated, we addressed the question whether PI3K or MAPK signaling is specifically activated by PDGF in EMT-transformed cells. MIM-ST, MIM-CT and MIM-RT cells were serum starved for 24 hours, stimulated for 30 minutes or 24 hours with PDGF and analyzed by Western blotting for Lamb1 and La levels as well as AKT and ERK activation (Figure 27). MIM-CT showed lower AKT, ERK, p-ERK and Lamb1 levels than MIM-ST and MIM-RT cells. Highest ERK activation was observed in MIM-ST cells. Interestingly, Lamb1 levels in MIM-ST were similar to MIM-RT. AKT activity increased after 30 minutes PDGF stimulation in MIM-CT cells only. In neither cell line p-ERK or Lamb1 levels changed upon treatment. Furthermore, cell lines showed similar La expression levels and besides the specific upper La band an additional lower band appeared in MIM-ST and MIM-RT cells. On the one hand these results propose that MAPK pathway is important upon EMT for Lamb1 expression, as MIM-ST, but not MIM-CT, showed similar Lamb1 levels as MIM-RT cells. On the other hand this experiment leads to the suggestion that PDGF signaling is neither AKT nor ERK-mediated because no activation was observed in MIM-RT. Taken together, these observations are not conclusive since MIM-

RT cells were previously capable for PDGF stimulation (Figure 23, Figure 26). Therefore further investigations are required to evaluate the role of these pathways upon PDGF treatment.

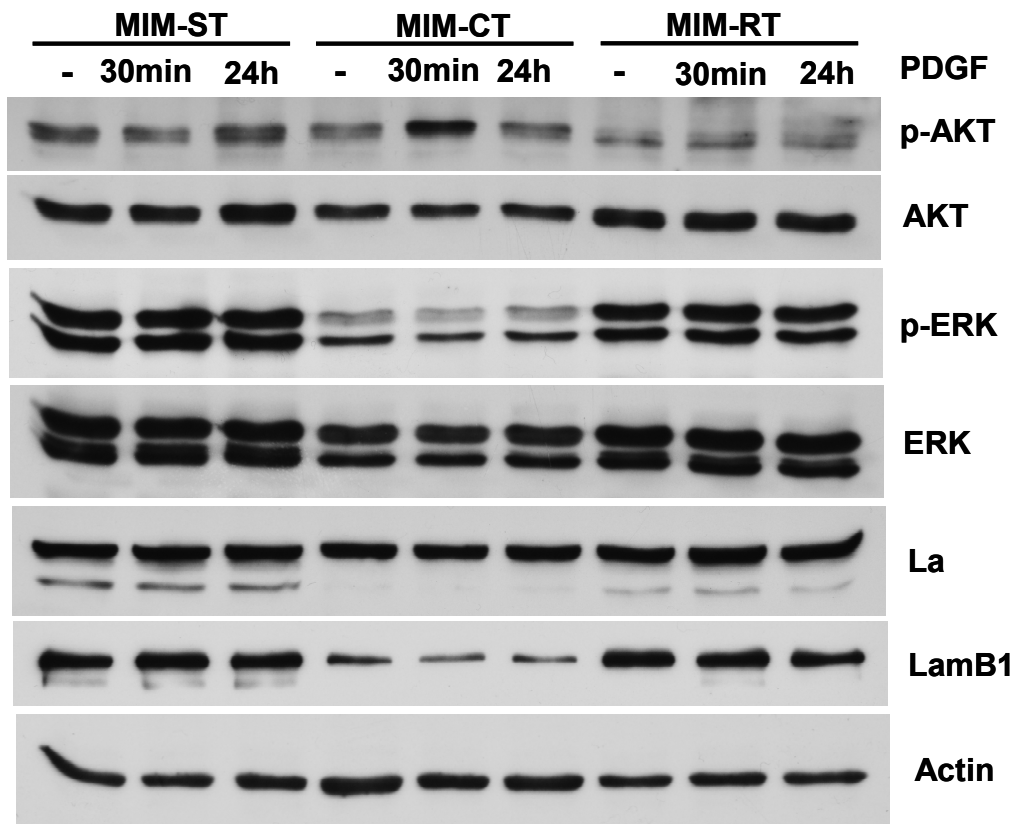


Figure 27 MIM-CT activates AKT upon PDGF treatment whereas MIM-ST as well as MIM-RT cells show no AKT or ERK response. MIM-ST, MIM-CT and MIM-RT cells were 24 hours serum starved and stimulated with PDGF for 30 minutes or 24 hours. Protein lysates were analyzed by Western blot for AKT and ERK activation as well as for La and Lamb1 levels.

7 DISCUSSION

TGF- β signaling induces EMT of murine hepatocytes in cooperation with constitutive active Ras, leading to enhanced MAPK and PI3K pathway activation [42]. Upon EMT, the ECM component LamB1 is translationally upregulated [100]. This upregulation results from increased activity of the IRES located in the 5'-UTR of LamB1 transcript [100]. The main purpose of the thesis was to understand how LamB1 IRES translation is controlled.

Since PI3K and MAPK is able to control translation we addressed the question whether one of them or even both are important for the activity of the LamB1 IRES [79]. We employed various malignant hepatocyte cell lines for our studies. MIM-R cells expresses constitutive active Ha-Ras whereas MIM-S35 and MIM-C40 cells express Ras mutants that selectively activate the MAPK or PI3K pathway in response to cognate signals, respectively [42]. LamB1 IRES activity was analyzed in untreated epithelial cells (MIM-S35, MIM-C40 and MIM-R), after initiating EMT by 24 hours TGF- β treatment and upon EMT transformation by long-term TGF- β treatment (MIM-ST, MIM-CT and MIM-RT) (Figure 18). Untreated epithelial cells showed similar levels of LamB1 IRES translation and 24 hours TGF- β treatment did not significantly increase LamB1 IRES activity. However, consistent with published findings, strong elevation of LamB1 IRES translation was observed in EMT-transformed cells [100]. These data points out that PI3K as well as MAPK pathway control LamB1 IRES translation. Though, upon EMT MAPK pathway seems to have a larger impact than PI3K pathway since MIM-ST showed higher LamB1 IRES levels than MIM-CT cells.

We further evaluated MAPK and PI3K signaling by analyzing their downstream targets ERK and AKT. Recently we found that La binds to the LamB1 IRES and controls its activity [101]. La in turn was reported to be regulated by AKT signaling in glial progenitors [129]. We therefore compared La and LamB1 protein levels in untreated MIM-S35, MIM-C40 and MIM-R cells, after 24 hours TGF- β treatment and in MIM-ST, MIM-CT and MIM-RT cells. Western blot analysis verified selective activation of PI3K and MAPK pathway in MIM-C40 and MIM-S35, respectively (Figure 19). Untreated MIM-C40 showed lowest LamB1 levels, which increased upon 24 hours TGF- β treatment. Notably, also p-ERK levels were elevated in 24 hours TGF- β treated MIM-C40 cells, leading to the suggestion that MAPK pathway is important for LamB1 expression in epithelial hepatocytes. Moreover, activation of AKT and ERK1/2 correlated with increased LamB1 expression upon EMT. This supports a regulatory role of PI3K and MAPK pathway in LamB1 translation. In addition, MIM-ST showed higher LamB1 levels than MIM-CT cells, which is in accordance with LamB1 IRES activities

(Figure 18), indicating a central role of MAPK pathway in the regulation of LamB1 expression upon EMT.

Furthermore, we used pharmacological inhibitors against PI3K and MAPK pathways to study their role in the regulation of LamB1 IRES translation. LamB1 IRES activity was analyzed in epithelial MIM-R and mesenchymal MIM-RT after inhibition of PI3K or MEK1/2 (Figure 20). Both inhibitors lead to a significant decrease of LamB1 IRES translation in MIM-R cells (Figure 20A). Interference with the PI3K pathway reduced LamB1 IRES activity to 50% and MEK1/2 inhibition led to a decrease by two thirds as compared to control. However, inhibitors had less effect in EMT-transformed cells (Figure 20B). After applying the PI3K inhibitor, LamB1 IRES activity was almost as high as in control cells and when inhibiting MEK1/2, 60% activity remained. On the one hand these results support a regulatory role of PI3K and MAPK pathway on LamB1 IRES. On the other hand these data show that LamB1 IRES is differently controlled between epithelial hepatocytes and EMT-transformed cells since inhibitors had different effects in MIM-R and MIM-RT cells. The PI3K and MAPK pathway regulate LamB1 IRES in MIM-R cells while in EMT-transformed MIM-RT some additional mechanisms might control LamB1 IRES translation.

We then assessed signaling after PI3K and MAPK pathway inhibition in MIM-R and MIM-RT cells by Western blotting (Figure 21). Decreased p-AKT or p-ERK levels confirmed inhibition of the PI3K or MAPK pathway, respectively. Interestingly, MIM-RT cells showed activation of MAPK signaling when PI3K pathway was inhibited and vice versa. This leads to the suggestion that upon EMT cells can bypass inhibition of the PI3K or MAPK pathway by activating the non-inhibited pathway. La expression did not change upon inhibition, in addition to the specific upper La band, a lower band appeared in all cells except the one after MEK1/2 inhibition. This additional band could be a cleaved or phosphorylated variant of La, which is inhibited after interfering with MAPK pathway. Consistent with earlier findings, EMT-transformed MIM-RT control cells expressed higher LamB1 levels than epithelial MIM-R control cells [100]. Interference with PI3K signaling influenced LamB1 levels in neither cell line. Moreover inhibition of MAPK pathway did not alter LamB1 levels in MIM-RT cells. On the contrary, levels were strongly decreased in MIM-R, suggesting that MEK1/2 inhibition is sufficient to block LamB1 expression. In summary, bicistronic assays and Western blotting (Figure 20, Figure 21) propose that the MAPK pathway is necessary for LamB1 IRES translation in epithelial hepatocytes and that both pathways can activate IRES translation upon EMT. Notably, a further possibility is that neither MAPK nor PI3K pathway influence LamB1 IRES translation in EMT-transformed cells.

We therefore addressed the question whether MIM-RT cells are sensitive to the combined inhibition of PI3K and MAPK pathway. LamB1 IRES activity was analyzed in mesenchymal MIM-RT cells after inhibition of PI3K and MEK1/2 (Figure 22A). Combined interference significantly reduced LamB1 IRES activity to two thirds as compared to control. Taken together results propose that PI3K as well as MAPK pathway regulate LamB1 IRES translation (Figure 20B, Figure 22A). The effect of PI3K and MAPK pathway inhibition on the signaling in MIM-RT cells was analyzed by Western blotting (Figure 22B). Decreased p-AKT and p-ERK levels confirmed inhibition of the PI3K or MAPK pathway. Interestingly, MIM-RT showed reduced LamB1 protein levels upon combined inhibition. These findings of bicistronic assays and Western blotting (Figure 22) corroborate the suggestion that upon EMT PI3K and MAPK regulate LamB1 IRES translation and that cells can bypass inhibition of one pathway alone by activating the non-inhibited pathway.

We further performed experiments to identify additional signaling pathways that are able to control LamB1 IRES translation upon EMT through AKT and ERK activation. Serum starved MIM-R and MIM-RT cells were stimulated with FCS, TGF- α , insulin or PDGF and analyzed by Western blotting (Figure 23). The results indicate that MIM-R and MIM-RT response to FCS, TGF- α and insulin, but only MIM-RT to PDGF. Interestingly it was previously described that EMT leads to an autocrine activation of PDGF signaling in murine MIM-RT hepatocytes [44]. We therefore determined PDGF ligand and receptor expression in different hepatic MIM cell lines by RT-PCR (Figure 24). The results revealed that PDGF signaling is increased not only in MIM-RT cells but also in all other EMT-transformed cell lines.

As mentioned earlier, La was found to bind and regulate LamB1 IRES [101]. In hepatocellular EMT, total La protein expression levels did not vary (Figure 13A). However, we observed that most of La is located in the nucleus in MIM-R and that La accumulates in the cytoplasm upon TGF- β treatment as well as EMT (Figure 13B). Moreover, it was reported that cytoplasmic La translocation is regulated by PDGF [129]. Since PDGF signaling increased during EMT we investigated the possible role of PDGF on La translocation.

Michaela Petz stimulated MIM-R, MIM-RT as well as corresponding MIM cells that express dominant negative PDGF-R α (MIM-R-dnP and MIM-RT-dnP) with PDGF and analyzed cytoplasmic and nuclear fractions by Western blotting (Figure 25). Results show that PDGF positively regulates cytoplasmic La localization and LamB1 expression upon hepatocellular EMT. These data also propose that probably an additional, PDGF-independent, pathway regulates La translocation and LamB1 expression since MIM-RT-dnP cells displayed higher LamB1 levels and cytoplasmic La compared to epithelial MIM-R-dnP.

We then assessed the direct effect of PDGF on LamB1 IRES translation upon EMT by performing bicistronic assays in PDGF-stimulated MIM-RT and -RT-dnP (Figure 26). TGF- β signaling was inhibited in these assays in order to block TGF- β -mediated autocrine PDGF signaling. Inhibition of TGF- β signaling did not decrease LamB1 IRES activity in untreated MIM-RT cells. We would have expected a decrease since TGF- β is important for autocrine PDGF signaling and EMT. Possible explanations could be that TGF- β inhibition induces stress and thereby a TGF- β independent pathway maintains IRES activity. Untreated MIM-RT had a higher LamB1 IRES activity than MIM-RT-dnP, which already indicates a regulatory role of PDGF in LamB1 IRES translation. More importantly, PDGF stimulation resulted in elevated LamB1 IRES activity in MIM-RT cells treated with TGF- β -RI/II inhibitor, suggesting that PDGF positively regulates the LamB1 IRES. Taken together, these results indicate that PDGF signaling enhances LamB1 IRES activity by regulating cytoplasmic La localization upon EMT.

To evaluate whether PDGF particularly activates the PI3K or MAPK pathway upon EMT we stimulated serum starved MIM-ST, MIM-CT and MIM-RT cells with PDGF and analyzed the downstream targets AKT and ERK by Western blotting (Figure 27). MIM-ST and MIM-CT are derived from epithelial MIM-S35 and MIM-C40 which selectively activate MAPK or PI3K pathway in response to cognate signals, respectively [42]. MIM-ST, MIM-CT and MIM-RT showed similar La levels. Moreover a second lower band appeared in MIM-ST and MIM-RT in addition to the specific upper La band. This observation fits to Figure 21, where interference of MAPK pathway inhibited this second band and to Figure 19, where MIM-ST showed highest expression of the second La band. Hence, this second band might be a differently modified, for instance cleaved or phosphorylated, variant of La, which is induced by MAPK pathway. Investigations to characterize this second La band would be an interesting task for future studies. Consistent with Figure 19, MIM-ST, but not MIM-CT, showed similar LamB1 levels as MIM-RT cells, suggesting that MAPK regulates LamB1 expression upon EMT. Additionally, only MIM-CT showed AKT activation, which further supports MAPK pathway in regulating LamB1 expression. However, neither AKT nor ERK activation upon stimulation was observed in MIM-ST and MIM-RT cells. Thus, these data lead to the suggestion that PDGF signals not via MAPK or PI3K pathway in EMT-transformed cells. These observations are contrary to previous findings where MIM-RT cells were capable for PDGF stimulation (Figure 23, Figure 26). Therefore further investigations are necessary to understand the role of MAPK and PI3K pathway in PDGF signaling. Since unstimulated control cells showed high p-ERK levels, it would probably help to inhibit TGF-

β -mediated autocrine PDGF signaling before analyzing PDGF downstream pathways.

Furthermore it would be important to determine LamB1 IRES activity in MIM-ST, MIM-CT and MIM-RT cells upon PDGF stimulation.

Since La enhanced LamB1 IRES translation it would be of interest to further analyze its regulation. Cytoplasmic and nuclear fractions of cells that were treated with MEK1/2, PI3K or both inhibitors could identify the regulatory pathway for cytoplasmic La accumulation.

Possible phosphorylation and cleavage sites of La could be predicted and deletion experiments using green fluorescent protein (GFP)- La constructs could be used for analyzing shuttling and La localization *in vivo* [129]. MIM-La knock-down cells could be employed for this approach and LamB1 IRES activity could be measured besides La localization. Also cell-free experimental systems could be employed to identify minimal ITAFs and canonical initiation factors needed for LamB1 IRES translation [81]. An interesting task would be to analyze LamB1 IRES activity *in vivo* under different conditions. Upon stable transduction of MIM cells with a construct harboring the LamB1 5'-UTR upstream of a luciferase reporter and cell injection into mice, luciferase expression could be detected in living animals by charged-couple device cameras [140].

A final model for the regulation of LamB1 IRES translation is displayed in Figure 28.

Epithelial MIM-R hepatocytes express constitutive active Ras, which is able to signal via MAPK or PI3K pathway without additional stimuli [42]. The MAPK pathway predominantly regulates LamB1 IRES translation and cytoplasmic La binds the LamB1 IRES to induce translation [101]. Long-term TGF- β treatment of MIM-R cells induces EMT, which leads to an activation of autocrine PDGF signaling [44]. This elevates MAPK as well as PI3K signaling and cytoplasmic La levels increase, thereby upregulating the IRES-mediated translation of LamB1 [42, 101]. The inhibition of MAPK pathway is sufficient to block LamB1 IRES translation in epithelial cells, whereas EMT-transformed cells are able to bypass inhibition of a single pathway. However, the MAPK pathway seems to be the primary regulatory mechanism also in EMT transformed cells. In addition a second, La-mediated but PDGF-independent, regulation is suggested to influence LamB1 IRES translation in EMT-transformed cells. Regulation of cytoplasmic La could be mediated by direct cytoplasmic localization of newly synthesized La or translocation of nuclear La to the cytoplasm. Possible modes of regulation for the latter one include protease cleavage where the NLS is removed and (de)phosphorylation of nuclear La. Phosphorylation of nuclear La by ERK1/2 or AKT seems likely since MAPK and PI3K pathway transduce their signals via phosphorylation.

Furthermore, AKT was shown to phosphorylate La, which leads to La translocation to the cytoplasm in glial progenitors [129].

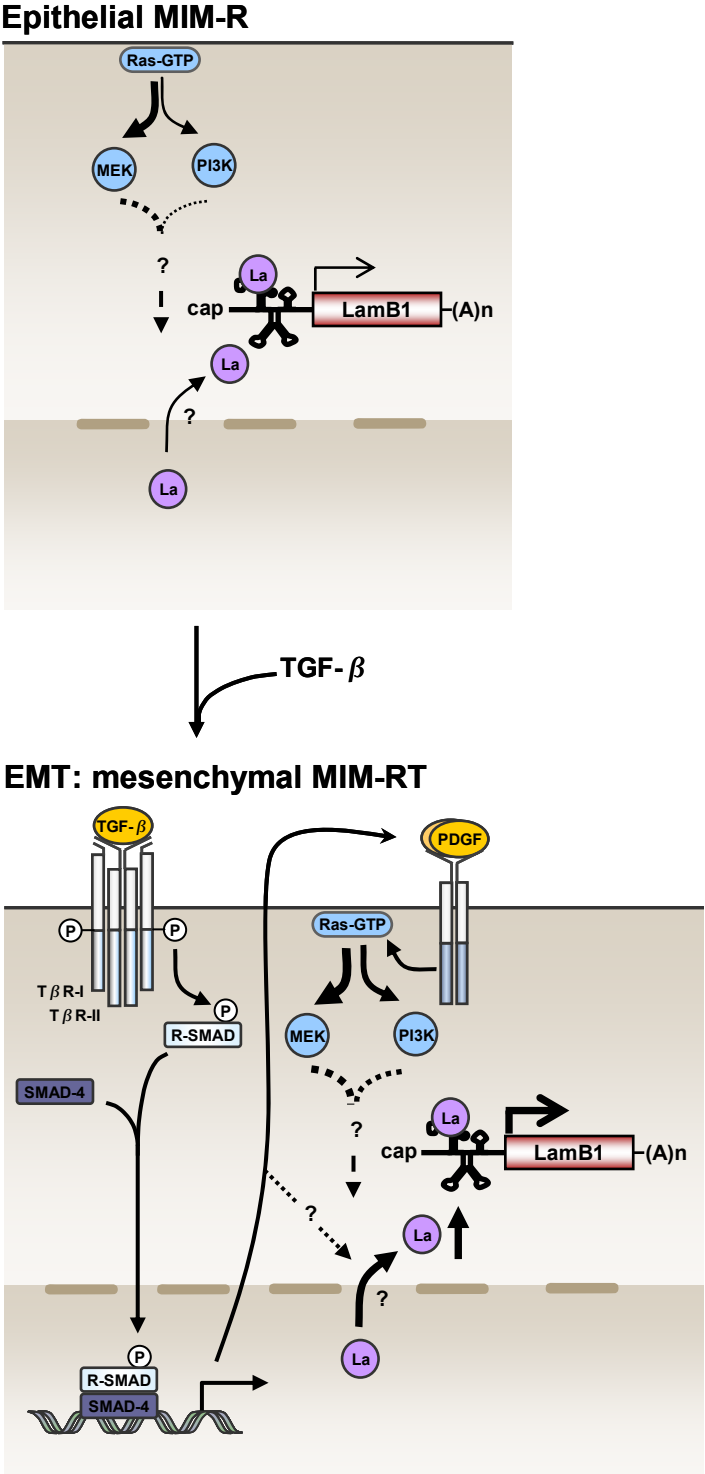


Figure 28 Suggested regulation of LamB1 IRES translation during hepatocellular EMT. Constitutive active Ras transduces signals via MAPK or PI3K pathway independently of stimuli [42]. LamB1 IRES translation is mainly controlled by MAPK signaling and binding of cytoplasmic La to its IRES [101]. Long-term TGF- β treatment of MIM-R cells leads to EMT,

which activates autocrine PDGF signaling [44]. MAPK and PI3K signaling as well as cytoplasmic La increases, which in turn upregulates LamB1 IRES translation [42, 101]. Moreover, a second La-mediated but PDGF-independent, pathway could be involved in the regulation of LamB1 IRES translation in EMT-transformed cells. Phosphorylation and subsequent translocation of La to the cytoplasm could regulate cytoplasmic La accumulation.

7.1 Concluding remarks and future perspectives

EMT is involved in invasion and metastasis, which is one hallmark of cancer and is associated with poor prognosis [10, 19, 20]. Several mechanisms were described to control EMT, such as upregulation of TGF- β signaling and transcriptional repression of E-cadherin [22].

Conversion of polarized epithelial cells to spindle-like mesenchymal cells and increased migratory potential are characteristics of EMT [9]. Interestingly, we found an IRES-mediated translational upregulation of LamB1 upon hepatocellular EMT [100]. In epithelial hepatocytes, the MAPK pathway controls the LamB1 IRES. Upon hepatocellular EMT, activated PDGF signaling and cytoplasmic La accumulation enhances LamB1 IRES translation. To our knowledge, these findings display a new mode of regulation upon EMT. Notably, IRES-mediated translation is important during conditions when cap-dependent translation is downregulated such as during angiogenesis, cell proliferation and apoptosis [81]. These processes are known to be important during cancer progression [87]. We suggest a possible involvement of LamB1 IRES-mediated translation in tumor progression. LamB1 is the β -subunit of several laminins and it has been reported to influence integrin-mediated cell migration and differentiation [102, 114]. It furthermore binds to LamR, which affects tumor invasion and metastasis [116, 117]. Therefore, a possible role of LamB1 during tumor progression could be the regulation of tumor cell migration and invasion. Angiogenesis is regulated by IRES-mediated translation of HIF-1 α , VEGF-A, PDGF-B [71, 94, 141]. Interestingly, LamB1 is involved in endothelial cell adhesion, tube formation and aortic sprouting [115]. Additionally, we observed that PDGF signaling enhances LamB1 IRES translation in our hepatocellular model. Thus, another role of LamB1 could be regulating tumor angiogenesis, which is induced by hypoxia during tumor progression [71, 94, 141]. PDGF signaling is involved in at least three hallmarks of cancer, namely self-sufficiency in growth signals, sustained angiogenesis as well as invasion and metastasis [19, 65]. In our EMT model, TGF- β leads to an autocrine PDGF signaling that supports tumor progression and LamB1 IRES translation [44]. A recent study compared extracellular matrix components in hepatocarcinogenesis and found LamB1 specifically upregulated in tumors of mice with

liver-specific transgenic expression of PDGF-C [142]. This observation further underlines a PDGF-dependent role of LamB1 in tumor progression.

Downstream pathways of PDGF include the PI3K and MAPK pathway, which regulate LamB1 IRES translation [67]. Notably, the latter one is suggested to be the main regulatory pathway in our hepatocellular EMT model [42]. Both pathways are known to regulate translation and are frequently altered in cancer [79]. Interestingly, it was shown that tumors with coexistent mutations in PI3K and MAPK pathway are insensitive to inhibition of either pathway alone but are sensitive to their combined inhibition [143]. Furthermore, 4E-BP1 was identified as a key downstream target of MAPK and PI3K pathway [143]. Another study revealed that human tumors with mutations in MAPK and PI3K pathway were insensitive to MEK inhibition, which normally leads to decreased cyclin D1 expression [144]. Notably, also cyclin D1 contains an IRES that is positively regulated by La [133]. In line with these observations, our results propose that EMT-transformed cells bypass inhibition of PI3K or MAPK pathway by activating the non-inhibited pathway. Hence, it could be that both pathways are able to control LamB1 IRES translation, probably through a shared downstream target. These findings are of relevance for treatment of cancer patients since inhibition of both pathways under certain conditions could impede tumor progression. Moreover, interference with La function would be an interesting therapeutic target as LamB1 IRES translation was enhanced by cytoplasmic La accumulation upon EMT [101]. However, as La is highly abundant and multifunctional, many side effects are likely after intervention [121]. Thus, understanding mechanistic modes of IRES translation will help to design new therapies in diseases like cancer. Accordingly, it will be of interest to dissect the function of LamB1 IRES translation upon hepatocellular EMT.

8 REFERENCES

1. Thompson, E.W., D.F. Newgreen, and D. Tarin, *Carcinoma invasion and metastasis: a role for epithelial-mesenchymal transition?* *Cancer Res*, 2005. **65**(14): p. 5991-5; discussion 5995.
2. Alberts, B., et al., *Molecular Biology of the Cell*. 2008, Garland Science Taylor&Francis Group. p. 1164-1169.
3. Kim, S.H., J. Turnbull, and S. Guimond, *Extracellular matrix and cell signalling: the dynamic cooperation of integrin, proteoglycan and growth factor receptor*. *J Endocrinol*. **209**(2): p. 139-51.
4. Alberts, B., et al., *Molecular Biology of the Cell*. 2008, Garland Science Taylor&Francis Group. p. 1131-1164.
5. Baum, B. and M. Georgiou, *Dynamics of adherens junctions in epithelial establishment, maintenance, and remodeling*. *J Cell Biol*. **192**(6): p. 907-17.
6. Stokes, D.L., *Desmosomes from a structural perspective*. *Curr Opin Cell Biol*, 2007. **19**(5): p. 565-71.
7. Berx, G. and F. van Roy, *Involvement of members of the cadherin superfamily in cancer*. *Cold Spring Harb Perspect Biol*, 2009. **1**(6): p. a003129.
8. van Zijl, F., G. Krupitza, and W. Mikulits, *Initial steps of metastasis: Cell invasion and endothelial transmigration*. *Mutat Res*.
9. Thiery, J.P. and J.P. Sleeman, *Complex networks orchestrate epithelial-mesenchymal transitions*. *Nat Rev Mol Cell Biol*, 2006. **7**(2): p. 131-42.
10. Thiery, J.P., et al., *Epithelial-mesenchymal transitions in development and disease*. *Cell*, 2009. **139**(5): p. 871-90.
11. Ciruna, B. and J. Rossant, *FGF signaling regulates mesoderm cell fate specification and morphogenetic movement at the primitive streak*. *Dev Cell*, 2001. **1**(1): p. 37-49.
12. Sauka-Spengler, T. and M. Bronner-Fraser, *A gene regulatory network orchestrates neural crest formation*. *Nat Rev Mol Cell Biol*, 2008. **9**(7): p. 557-68.
13. Timmerman, L.A., et al., *Notch promotes epithelial-mesenchymal transition during cardiac development and oncogenic transformation*. *Genes Dev*, 2004. **18**(1): p. 99-115.
14. Savagner, P., et al., *Developmental transcription factor slug is required for effective re-epithelialization by adult keratinocytes*. *J Cell Physiol*, 2005. **202**(3): p. 858-66.
15. Liu, Y., *New insights into epithelial-mesenchymal transition in kidney fibrosis*. *J Am Soc Nephrol*. **21**(2): p. 212-22.
16. Lopez-Novoa, J.M. and M.A. Nieto, *Inflammation and EMT: an alliance towards organ fibrosis and cancer progression*. *EMBO Mol Med*, 2009. **1**(6-7): p. 303-14.
17. Mani, S.A., et al., *The epithelial-mesenchymal transition generates cells with properties*

- of stem cells*. Cell, 2008. **133**(4): p. 704-15.
18. Wellner, U., et al., *The EMT-activator ZEB1 promotes tumorigenicity by repressing stemness-inhibiting microRNAs*. Nat Cell Biol, 2009. **11**(12): p. 1487-95.
 19. Hanahan, D. and R.A. Weinberg, *The hallmarks of cancer*. Cell, 2000. **100**(1): p. 57-70.
 20. Sporn, M.B., *The war on cancer*. Lancet, 1996. **347**(9012): p. 1377-81.
 21. Friedl, P. and K. Wolf, *Tumour-cell invasion and migration: diversity and escape mechanisms*. Nat Rev Cancer, 2003. **3**(5): p. 362-74.
 22. Thiery, J.P., *Epithelial-mesenchymal transitions in tumour progression*. Nat Rev Cancer, 2002. **2**(6): p. 442-54.
 23. Giampieri, S., et al., *Localized and reversible TGFbeta signalling switches breast cancer cells from cohesive to single cell motility*. Nat Cell Biol, 2009. **11**(11): p. 1287-96.
 24. Ansieau, S., et al., *Induction of EMT by twist proteins as a collateral effect of tumor-promoting inactivation of premature senescence*. Cancer Cell, 2008. **14**(1): p. 79-89.
 25. Yang, A.D., et al., *Chronic oxaliplatin resistance induces epithelial-to-mesenchymal transition in colorectal cancer cell lines*. Clin Cancer Res, 2006. **12**(14 Pt 1): p. 4147-53.
 26. Moustakas, A. and C.H. Heldin, *Signaling networks guiding epithelial-mesenchymal transitions during embryogenesis and cancer progression*. Cancer Sci, 2007. **98**(10): p. 1512-20.
 27. Valles, A.M., et al., *Acidic fibroblast growth factor is a modulator of epithelial plasticity in a rat bladder carcinoma cell line*. Proc Natl Acad Sci U S A, 1990. **87**(3): p. 1124-8.
 28. Zoltan-Jones, A., et al., *Elevated hyaluronan production induces mesenchymal and transformed properties in epithelial cells*. J Biol Chem, 2003. **278**(46): p. 45801-10.
 29. Birchmeier, C., et al., *Met, metastasis, motility and more*. Nat Rev Mol Cell Biol, 2003. **4**(12): p. 915-25.
 30. Larue, L. and A. Bellacosa, *Epithelial-mesenchymal transition in development and cancer: role of phosphatidylinositol 3' kinase/AKT pathways*. Oncogene, 2005. **24**(50): p. 7443-54.
 31. Wang, Z., et al., *The role of Notch signaling pathway in epithelial-mesenchymal transition (EMT) during development and tumor aggressiveness*. Curr Drug Targets. **11**(6): p. 745-51.
 32. Gregory, P.A., et al., *MicroRNAs as regulators of epithelial-mesenchymal transition*. Cell Cycle, 2008. **7**(20): p. 3112-8.
 33. Yang, M.H., et al., *Direct regulation of TWIST by HIF-1alpha promotes metastasis*. Nat Cell Biol, 2008. **10**(3): p. 295-305.
 34. Peinado, H., F. Portillo, and A. Cano, *Transcriptional regulation of cadherins during development and carcinogenesis*. Int J Dev Biol, 2004. **48**(5-6): p. 365-75.

35. Berx, G., et al., *Mutations of the human E-cadherin (CDH1) gene*. Hum Mutat, 1998. **12**(4): p. 226-37.
36. Valles, A.M., et al., *Alpha 2 beta 1 integrin is required for the collagen and FGF-1 induced cell dispersion in a rat bladder carcinoma cell line*. Cell Adhes Commun, 1996. **4**(3): p. 187-99.
37. El-Serag, H.B. and K.L. Rudolph, *Hepatocellular carcinoma: epidemiology and molecular carcinogenesis*. Gastroenterology, 2007. **132**(7): p. 2557-76.
38. Llovet, J.M., A. Burroughs, and J. Bruix, *Hepatocellular carcinoma*. Lancet, 2003. **362**(9399): p. 1907-17.
39. Sun, V.C. and L. Sarna, *Symptom management in hepatocellular carcinoma*. Clin J Oncol Nurs, 2008. **12**(5): p. 759-66.
40. Zhai, B., et al., *Reduced expression of E-cadherin/catenin complex in hepatocellular carcinomas*. World J Gastroenterol, 2008. **14**(37): p. 5665-73.
41. Giannelli, G., et al., *Laminin-5 with transforming growth factor-beta1 induces epithelial to mesenchymal transition in hepatocellular carcinoma*. Gastroenterology, 2005. **129**(5): p. 1375-83.
42. Fischer, A.N., et al., *Integration of Ras subeffector signaling in TGF-beta mediated late stage hepatocarcinogenesis*. Carcinogenesis, 2005. **26**(5): p. 931-42.
43. Mikula, M., et al., *Immortalized p19ARF null hepatocytes restore liver injury and generate hepatic progenitors after transplantation*. Hepatology, 2004. **39**(3): p. 628-34.
44. Gotzmann, J., et al., *A crucial function of PDGF in TGF-beta-mediated cancer progression of hepatocytes*. Oncogene, 2006. **25**(22): p. 3170-85.
45. Blobe, G.C., W.P. Schiemann, and H.F. Lodish, *Role of transforming growth factor beta in human disease*. N Engl J Med, 2000. **342**(18): p. 1350-8.
46. Ikushima, H. and K. Miyazono, *TGFbeta signalling: a complex web in cancer progression*. Nat Rev Cancer. **10**(6): p. 415-24.
47. Shi, Y. and J. Massague, *Mechanisms of TGF-beta signaling from cell membrane to the nucleus*. Cell, 2003. **113**(6): p. 685-700.
48. Rifkin, D.B., *Latent transforming growth factor-beta (TGF-beta) binding proteins: orchestrators of TGF-beta availability*. J Biol Chem, 2005. **280**(9): p. 7409-12.
49. Zhang, Y.E., *Non-Smad pathways in TGF-beta signaling*. Cell Res, 2009. **19**(1): p. 128-39.
50. Levy, L. and C.S. Hill, *Alterations in components of the TGF-beta superfamily signaling pathways in human cancer*. Cytokine Growth Factor Rev, 2006. **17**(1-2): p. 41-58.
51. Datto, M.B., et al., *Transforming growth factor beta induces the cyclin-dependent kinase inhibitor p21 through a p53-independent mechanism*. Proc Natl Acad Sci U S A, 1995. **92**(12): p. 5545-9.

52. Yagi, K., et al., *c-myc is a downstream target of the Smad pathway*. J Biol Chem, 2002. **277**(1): p. 854-61.
53. Deheuninck, J. and K. Luo, *Ski and SnoN, potent negative regulators of TGF-beta signaling*. Cell Res, 2009. **19**(1): p. 47-57.
54. Jang, C.W., et al., *TGF-beta induces apoptosis through Smad-mediated expression of DAP-kinase*. Nat Cell Biol, 2002. **4**(1): p. 51-8.
55. Kiyono, K., et al., *Autophagy is activated by TGF-beta and potentiates TGF-beta-mediated growth inhibition in human hepatocellular carcinoma cells*. Cancer Res, 2009. **69**(23): p. 8844-52.
56. Komuro, A., et al., *Diffuse-type gastric carcinoma: progression, angiogenesis, and transforming growth factor beta signaling*. J Natl Cancer Inst, 2009. **101**(8): p. 592-604.
57. Battegay, E.J., et al., *TGF-beta induces bimodal proliferation of connective tissue cells via complex control of an autocrine PDGF loop*. Cell, 1990. **63**(3): p. 515-24.
58. Sintich, S.M., et al., *Transforming growth factor-beta1-induced proliferation of the prostate cancer cell line, TSU-Pr1: the role of platelet-derived growth factor*. Endocrinology, 1999. **140**(8): p. 3411-5.
59. Ehata, S., et al., *Transforming growth factor-beta promotes survival of mammary carcinoma cells through induction of antiapoptotic transcription factor DECI*. Cancer Res, 2007. **67**(20): p. 9694-703.
60. Iwasaki, H. and T. Suda, *Cancer stem cells and their niche*. Cancer Sci, 2009. **100**(7): p. 1166-72.
61. Sanchez-Elsner, T., et al., *Synergistic cooperation between hypoxia and transforming growth factor-beta pathways on human vascular endothelial growth factor gene expression*. J Biol Chem, 2001. **276**(42): p. 38527-35.
62. Xu, J., S. Lamouille, and R. Derynck, *TGF-beta-induced epithelial to mesenchymal transition*. Cell Res, 2009. **19**(2): p. 156-72.
63. Araki, S., et al., *TGF-beta1-induced expression of human Mdm2 correlates with late-stage metastatic breast cancer*. J Clin Invest. **120**(1): p. 290-302.
64. Bierie, B. and H.L. Moses, *Tumour microenvironment: TGFbeta: the molecular Jekyll and Hyde of cancer*. Nat Rev Cancer, 2006. **6**(7): p. 506-20.
65. Andrae, J., R. Gallini, and C. Betsholtz, *Role of platelet-derived growth factors in physiology and medicine*. Genes Dev, 2008. **22**(10): p. 1276-312.
66. Heldin, C.H. and B. Westermark, *Mechanism of action and in vivo role of platelet-derived growth factor*. Physiol Rev, 1999. **79**(4): p. 1283-316.
67. Heldin, C.H., A. Ostman, and L. Ronnstrand, *Signal transduction via platelet-derived growth factor receptors*. Biochim Biophys Acta, 1998. **1378**(1): p. F79-113.
68. Sultzman, L., et al., *Platelet-derived growth factor increases the in vivo activity of*

- phospholipase C-gamma 1 and phospholipase C-gamma 2*. Mol Cell Biol, 1991. **11**(4): p. 2018-25.
69. Hu, Q., et al., *Ras-dependent induction of cellular responses by constitutively active phosphatidylinositol-3 kinase*. Science, 1995. **268**(5207): p. 100-2.
 70. Coughlin, S.R., J.A. Escobedo, and L.T. Williams, *Role of phosphatidylinositol kinase in PDGF receptor signal transduction*. Science, 1989. **243**(4895): p. 1191-4.
 71. Rosmorduc, O. and C. Housset, *Hypoxia: a link between fibrogenesis, angiogenesis, and carcinogenesis in liver disease*. Semin Liver Dis. **30**(3): p. 258-70.
 72. Furuhashi, M., et al., *Platelet-derived growth factor production by B16 melanoma cells leads to increased pericyte abundance in tumors and an associated increase in tumor growth rate*. Cancer Res, 2004. **64**(8): p. 2725-33.
 73. Xian, X., et al., *Pericytes limit tumor cell metastasis*. J Clin Invest, 2006. **116**(3): p. 642-51.
 74. Dong, J., et al., *VEGF-null cells require PDGFR alpha signaling-mediated stromal fibroblast recruitment for tumorigenesis*. EMBO J, 2004. **23**(14): p. 2800-10.
 75. Karnoub, A.E., et al., *Mesenchymal stem cells within tumour stroma promote breast cancer metastasis*. Nature, 2007. **449**(7162): p. 557-63.
 76. Orimo, A., et al., *Stromal fibroblasts present in invasive human breast carcinomas promote tumor growth and angiogenesis through elevated SDF-1/CXCL12 secretion*. Cell, 2005. **121**(3): p. 335-48.
 77. Yang, L., C. Lin, and Z.R. Liu, *P68 RNA helicase mediates PDGF-induced epithelial mesenchymal transition by displacing Axin from beta-catenin*. Cell, 2006. **127**(1): p. 139-55.
 78. Rodnina, M.V. and W. Wintermeyer, *Recent mechanistic insights into eukaryotic ribosomes*. Curr Opin Cell Biol, 2009. **21**(3): p. 435-43.
 79. Silvera, D., S.C. Formenti, and R.J. Schneider, *Translational control in cancer*. Nat Rev Cancer. **10**(4): p. 254-66.
 80. Sonenberg, N. and A.G. Hinnebusch, *Regulation of translation initiation in eukaryotes: mechanisms and biological targets*. Cell, 2009. **136**(4): p. 731-45.
 81. Komar, A.A. and M. Hatzoglou, *Cellular IRES-mediated translation: the war of ITAFs in pathophysiological states*. Cell Cycle. **10**(2): p. 229-40.
 82. Zetterberg, A., O. Larsson, and K.G. Wiman, *What is the restriction point?* Curr Opin Cell Biol, 1995. **7**(6): p. 835-42.
 83. Ruggero, D., et al., *The translation factor eIF-4E promotes tumor formation and cooperates with c-Myc in lymphomagenesis*. Nat Med, 2004. **10**(5): p. 484-6.
 84. Coleman, L.J., et al., *Combined analysis of eIF4E and 4E-binding protein expression predicts breast cancer survival and estimates eIF4E activity*. Br J Cancer, 2009. **100**(9):

- p. 1393-9.
85. Pelletier, J., et al., *Cap-independent translation of poliovirus mRNA is conferred by sequence elements within the 5' noncoding region*. Mol Cell Biol, 1988. **8**(3): p. 1103-12.
 86. Spahn, C.M., et al., *Cryo-EM visualization of a viral internal ribosome entry site bound to human ribosomes: the IRES functions as an RNA-based translation factor*. Cell, 2004. **118**(4): p. 465-75.
 87. Holcik, M., *Targeting translation for treatment of cancer--a novel role for IRES?* Curr Cancer Drug Targets, 2004. **4**(3): p. 299-311.
 88. Prevot, D., J.L. Darlix, and T. Ohlmann, *Conducting the initiation of protein synthesis: the role of eIF4G*. Biol Cell, 2003. **95**(3-4): p. 141-56.
 89. Spriggs, K.A., et al., *Canonical initiation factor requirements of the Myc family of internal ribosome entry segments*. Mol Cell Biol, 2009. **29**(6): p. 1565-74.
 90. Allam, H. and N. Ali, *Initiation factor eIF2-independent mode of c-Src mRNA translation occurs via an internal ribosome entry site*. J Biol Chem. **285**(8): p. 5713-25.
 91. Stoneley, M. and A.E. Willis, *Cellular internal ribosome entry segments: structures, trans-acting factors and regulation of gene expression*. Oncogene, 2004. **23**(18): p. 3200-7.
 92. Komar, A.A. and M. Hatzoglou, *Internal ribosome entry sites in cellular mRNAs: mystery of their existence*. J Biol Chem, 2005. **280**(25): p. 23425-8.
 93. Lewis, S.M. and M. Holcik, *For IRES trans-acting factors, it is all about location*. Oncogene, 2008. **27**(8): p. 1033-5.
 94. Braunstein, S., et al., *A hypoxia-controlled cap-dependent to cap-independent translation switch in breast cancer*. Mol Cell, 2007. **28**(3): p. 501-12.
 95. Shi, Y., et al., *IL-6-induced stimulation of c-myc translation in multiple myeloma cells is mediated by myc internal ribosome entry site function and the RNA-binding protein, hnRNP A1*. Cancer Res, 2008. **68**(24): p. 10215-22.
 96. Holcik, M., et al., *Translational upregulation of X-linked inhibitor of apoptosis (XIAP) increases resistance to radiation induced cell death*. Oncogene, 2000. **19**(36): p. 4174-7.
 97. Weinberg, R.A., *The Biology of Cancer*. 2007, Garland Science Taylor&Francis Group. p. 173-176.
 98. Waskiewicz, A.J., et al., *Mitogen-activated protein kinases activate the serine/threonine kinases Mnk1 and Mnk2*. EMBO J, 1997. **16**(8): p. 1909-20.
 99. Weinberg, R.A., *The Biology of Cancer*. 2007, Garland Science Taylor&Francis Group. p. 176-183.
 100. Petz, M., et al., *The leader region of Laminin B1 mRNA confers cap-independent translation*. Nucleic Acids Res, 2007. **35**(8): p. 2473-82.

101. Petz, M., et al., *La enhances IRES-mediated translation of laminin B1 during malignant epithelial to mesenchymal transition*. Nucleic Acids Research, 2011. **in press**.
102. Alberts, B., et al., *Molecular Biology of the Cell*. 2008, Garland Science Taylor&Francis Group. p. 1165-1166.
103. Miner, J.H. and P.D. Yurchenco, *Laminin functions in tissue morphogenesis*. Annu Rev Cell Dev Biol, 2004. **20**: p. 255-84.
104. Durbeej, M., *Laminins*. Cell Tissue Res. **339**(1): p. 259-68.
105. Timpl, R., et al., *Structure and function of laminin LG modules*. Matrix Biol, 2000. **19**(4): p. 309-17.
106. Patarroyo, M., K. Tryggvason, and I. Virtanen, *Laminin isoforms in tumor invasion, angiogenesis and metastasis*. Semin Cancer Biol, 2002. **12**(3): p. 197-207.
107. Jimenez-Mallebrera, C., et al., *Congenital muscular dystrophy: molecular and cellular aspects*. Cell Mol Life Sci, 2005. **62**(7-8): p. 809-23.
108. Tzu, J. and M.P. Marinkovich, *Bridging structure with function: structural, regulatory, and developmental role of laminins*. Int J Biochem Cell Biol, 2008. **40**(2): p. 199-214.
109. Engbring, J.A. and H.K. Kleinman, *The basement membrane matrix in malignancy*. J Pathol, 2003. **200**(4): p. 465-70.
110. Klominek, J., K.H. Robert, and K.G. Sundqvist, *Chemotaxis and haptotaxis of human malignant mesothelioma cells: effects of fibronectin, laminin, type IV collagen, and an autocrine motility factor-like substance*. Cancer Res, 1993. **53**(18): p. 4376-82.
111. Castronovo, V., *Laminin receptors and laminin-binding proteins during tumor invasion and metastasis*. Invasion Metastasis, 1993. **13**(1): p. 1-30.
112. Delwel, G.O., et al., *Distinct and overlapping ligand specificities of the alpha 3A beta 1 and alpha 6A beta 1 integrins: recognition of laminin isoforms*. Mol Biol Cell, 1994. **5**(2): p. 203-15.
113. Kusuma, N., et al., *Integrin-dependent response to laminin-511 regulates breast tumor cell invasion and metastasis*. Int J Cancer.
114. Taniguchi, Y., et al., *The C-terminal region of laminin beta chains modulates the integrin binding affinities of laminins*. J Biol Chem, 2009. **284**(12): p. 7820-31.
115. Malinda, K.M., et al., *Identification of laminin alpha1 and beta1 chain peptides active for endothelial cell adhesion, tube formation, and aortic sprouting*. FASEB J, 1999. **13**(1): p. 53-62.
116. Massia, S.P., S.S. Rao, and J.A. Hubbell, *Covalently immobilized laminin peptide Tyr-Ile-Gly-Ser-Arg (YIGSR) supports cell spreading and co-localization of the 67-kilodalton laminin receptor with alpha-actinin and vinculin*. J Biol Chem, 1993. **268**(11): p. 8053-9.
117. Menard, S., E. Tagliabue, and M.I. Colnaghi, *The 67 kDa laminin receptor as a prognostic factor in human cancer*. Breast Cancer Res Treat, 1998. **52**(1-3): p. 137-45.

118. Vande Broek, I., et al., *Laminin-1-induced migration of multiple myeloma cells involves the high-affinity 67 kD laminin receptor*. Br J Cancer, 2001. **85**(9): p. 1387-95.
119. Alspaugh, M.A. and E.M. Tan, *Antibodies to cellular antigens in Sjogren's syndrome*. J Clin Invest, 1975. **55**(5): p. 1067-73.
120. Mattioli, M. and M. Reichlin, *Heterogeneity of RNA protein antigens reactive with sera of patients with systemic lupus erythematosus. Description of a cytoplasmic nonribosomal antigen*. Arthritis Rheum, 1974. **17**(4): p. 421-9.
121. Wolin, S.L. and T. Cedervall, *The La protein*. Annu Rev Biochem, 2002. **71**: p. 375-403.
122. Maraia, R.J. and M.A. Bayfield, *The La protein-RNA complex surfaces*. Mol Cell, 2006. **21**(2): p. 149-52.
123. Craig, A.W., et al., *The La autoantigen contains a dimerization domain that is essential for enhancing translation*. Mol Cell Biol, 1997. **17**(1): p. 163-9.
124. Ayukawa, K., et al., *La autoantigen is cleaved in the COOH terminus and loses the nuclear localization signal during apoptosis*. J Biol Chem, 2000. **275**(44): p. 34465-70.
125. Broekhuis, C.H., et al., *Detailed analysis of the phosphorylation of the human La (SS-B) autoantigen. (De)phosphorylation does not affect its subcellular distribution*. Biochemistry, 2000. **39**(11): p. 3023-33.
126. Shiroki, K., et al., *Intracellular redistribution of truncated La protein produced by poliovirus 3Cpro-mediated cleavage*. J Virol, 1999. **73**(3): p. 2193-200.
127. Simons, F.H., et al., *Characterization of cis-acting signals for nuclear import and retention of the La (SS-B) autoantigen*. Exp Cell Res, 1996. **224**(2): p. 224-36.
128. Hendrick, J.P., et al., *Ro small cytoplasmic ribonucleoproteins are a subclass of La ribonucleoproteins: further characterization of the Ro and La small ribonucleoproteins from uninfected mammalian cells*. Mol Cell Biol, 1981. **1**(12): p. 1138-49.
129. Brenet, F., et al., *Akt phosphorylation of La regulates specific mRNA translation in glial progenitors*. Oncogene, 2009. **28**(1): p. 128-39.
130. Meerovitch, K., et al., *La autoantigen enhances and corrects aberrant translation of poliovirus RNA in reticulocyte lysate*. J Virol, 1993. **67**(7): p. 3798-807.
131. Holcik, M. and R.G. Korneluk, *Functional characterization of the X-linked inhibitor of apoptosis (XIAP) internal ribosome entry site element: role of La autoantigen in XIAP translation*. Mol Cell Biol, 2000. **20**(13): p. 4648-57.
132. Kim, Y.K., et al., *La autoantigen enhances translation of BiP mRNA*. Nucleic Acids Res, 2001. **29**(24): p. 5009-16.
133. Sommer, G., et al., *The RNA-binding protein La contributes to cell proliferation and CCND1 expression*. Oncogene. **30**(4): p. 434-44.
134. Carter, M.S. and P. Sarnow, *Distinct mRNAs that encode La autoantigen are differentially expressed and contain internal ribosome entry sites*. J Biol Chem, 2000.

275(36): p. 28301-7.

135. Giehl, K., et al., *Growth factor-dependent activation of the Ras-Raf-MEK-MAPK pathway in the human pancreatic carcinoma cell line PANC-1 carrying activated K-ras: implications for cell proliferation and cell migration*. *Oncogene*, 2000. **19**(25): p. 2930-42.
136. Krystal, G.W., G. Sulanke, and J. Litz, *Inhibition of phosphatidylinositol 3-kinase-Akt signaling blocks growth, promotes apoptosis, and enhances sensitivity of small cell lung cancer cells to chemotherapy*. *Mol Cancer Ther*, 2002. **1**(11): p. 913-22.
137. Le Cras, T.D., et al., *Inhibition of PI3K by PX-866 prevents transforming growth factor-alpha-induced pulmonary fibrosis*. *Am J Pathol*. **176**(2): p. 679-86.
138. Mussig, K. and H.U. Haring, *Insulin signal transduction in normal cells and its role in carcinogenesis*. *Exp Clin Endocrinol Diabetes*. **118**(6): p. 356-9.
139. Oliver, B.L., R.I. Sha'afi, and J.J. Hajjar, *Transforming growth factor-alpha and epidermal growth factor activate mitogen-activated protein kinase and its substrates in intestinal epithelial cells*. *Proc Soc Exp Biol Med*, 1995. **210**(2): p. 162-70.
140. Obad, S., et al., *Silencing of microRNA families by seed-targeting tiny LNAs*. *Nat Genet*. **43**(4): p. 371-8.
141. Bernstein, J., et al., *PDGF2/c-sis mRNA leader contains a differentiation-linked internal ribosomal entry site (D-IRES)*. *J Biol Chem*, 1997. **272**(14): p. 9356-62.
142. Lai, K.K., et al., *Extracellular Matrix Dynamics in Hepatocarcinogenesis: a Comparative Proteomics Study of PDGFC Transgenic and Pten Null Mouse Models*. *PLoS Genet*. **7**(6): p. e1002147.
143. She, Q.B., et al., *4E-BP1 is a key effector of the oncogenic activation of the AKT and ERK signaling pathways that integrates their function in tumors*. *Cancer Cell*. **18**(1): p. 39-51.
144. Halilovic, E., et al., *PIK3CA mutation uncouples tumor growth and cyclin D1 regulation from MEK/ERK and mutant KRAS signaling*. *Cancer Res*. **70**(17): p. 6804-14.

9 ANNOTATION

Note that part of the data is included in a manuscript in preparation and in the PhD thesis of Michaela Petz.

10 CURRICULUM VITAE

Personal Data	
First name	Nicole
Last name	Them
Birthday	10 th May 1987
Birthplace	Vienna, Austria
E- Mail	nicole.them@gmail.com
Education	
1993- 1997	Elementary school, Vienna, Austria
1997- 2005	Real gymnasium, final exam passed with distinction, Vienna, Austria
October 2006- September 2011	Diploma studies of Molecular Biology (specialization in Cell Biology, Immunology and Molecular Medicine), Vienna, Austria
Job History	
August- September 2009	Internship at J. V. Small's Lab, IMBA, Vienna, Austria
September- December 2009	Internship at P. Kovarik's Lab, MFPL, Vienna, Austria
June 2010- August 2011	Internship and Diploma thesis at W. Mikulits's Lab, Institute of Cancer Research, Vienna, Austria
Other Activities	
January- June 2010	Erasmus term in Lund, Sweden
Scholarship	
December 2009	Erasmus scholarship by the University of Vienna for studying abroad
January 2010	For outstanding academic achievements by the University of Vienna
January 2011	For outstanding academic achievements by the University of Vienna
Publication	
2011	M. Petz, N. Them, H. Huber, H. Beug and W. Mikulits, <i>La enhances IRES-mediated translation of laminin B1 during malignant epithelial to mesenchymal transition.</i> Nucleic Acids Research, 2011. In press.

11 ACKNOWLEDGEMENTS

I would like to thank Wolfgang not only for the possibility to work as a Diploma student in his lab but also for his great supervision. I got the opportunity to learn new practical skills and work on a publication. I am very grateful for his confidence during my Diploma work, the effort he spent to correct my Diploma thesis and his immense support for my PhD application. A huge thank to Michi for her big supervision and the fruitful discussions on our interesting project. She provided assistance and guidance whenever needed. Furthermore, I appreciate her calmness and helpful input on my Diploma thesis.

I would like to say “thank you” to all my lab colleagues for their support and for this exciting year. A special thank to Heidi, she helped when I was struggling and not to forget to mention the delicious meals she prepared. Likewise I am grateful to Georg for his big support such as calculating statistics. Of course, many thanks to Markus, he assisted when I had practical problems and gave a critical and helpful input to the project. Furthermore, I am thankful to Alex for her support not only in the lab but also as a friend.

I would like to express my appreciation to my special friends Dagi, Mu, Susi, Bino and Flo. They were such a great help and made my Diploma studies in Molecular Biology to a time that I will never forget.

At the end, most heartfelt thanks to my family who always believed in me and supported me throughout my life. I am especially grateful to Dani for his love.